A general framework for two-photon spontaneous emission near plasmonic nanostructures

S. Smeets,* B. Maes,† and G. Rosolen‡
Micro- and Nanophotonic Materials Group, Research Institute for Materials Science and Engineering, University of Mons, 20 Place du Parc, Mons B-7000, Belgium
(Dated: June 5, 2023)

We present a general framework that computes the two-photon spontaneous emission rate of a quantum emitter close to an arbitrary photonic structure beyond the dipolar approximation. This is relevant for strongly confined light fields, such as in plasmonic nano- and picocavities, which are currently being explored to enhance higher-order light-matter interactions. In our framework, the emitter contribution to this process is calculated analytically, while the influence of the photonic environment is determined via the computation of Purcell factors with conventional electromagnetic simulations, which avoids tedious analytic calculations for the environment. Also, our framework efficiently handles asymmetric structures that were not treated before. We show that placing a hydrogen-like emitter close to a silver nanodisk enhances the transition rate between two spherically symmetric states by 5 and 11 orders of magnitude via electric dipole and quadrupole two-photon transitions, respectively. In the future, controlling this process promises efficient entangled two-photon sources for quantum applications, new platforms in spectroscopy, as well as broadband absorbers and emitters.

I. INTRODUCTION

Spontaneous emission, which is responsible for most of the light we see around us, is a fundamental process in the field of light-matter interaction. In this process, an excited quantum emitter (e.g., an atom, a molecule, or a quantum dot) decays into a lower energy state by emitting a quantized amount of energy in the form of a single quantum or in the form of several quanta [1–3]. These transitions are also responsible for the fingerprint of atoms and molecules, which is their emission spectrum [4].

Nowadays, it is well known that the spontaneous emission rate of an emitter does not depend only on the emitter itself but also on its environment, termed the Purcell effect [5, 6]. Moreover, an excited emitter can decay either radiatively in the case of photon emission in the far-field or non-radiatively in the case of energy dissipation in the environment in the form of, for example, phonons or plasmons [6]. Especially near metallic structures, the two relaxation channels can be enhanced [7], and in many applications one aims to harness the radiative one.

Usually, because the size of a quantum emitter is typically three orders of magnitude smaller than the wavelength of the emitted light, it is sufficient to study the influence of the environment on the emitter under the electric dipole approximation [6, 8]. In the latter approach the emitter feels a uniform electric field, thus neglecting the spatial variations of the field over it. Therefore, the emitter is assumed to be a point and only electric dipole transitions can occur [9], making most of the characteristic emitter transitions inaccessible [10].

Nevertheless, when the spatial extent of an emitter is no longer negligible compared to the wavelength of light, the point dipole approximation is no longer valid. This can happen with emitters having a large spatial extent, such as quantum dots or organic molecules [11–14] and in current devices used to increase light-matter interactions [15] where the light can be highly confined, such as photonic crystals [16, 17], plasmonic nanocavities [11, 18–22], nanomagnonic cavities [23, 24], and polar dielectrics [25, 26]. For example, the wavelength can be squeezed by two orders of magnitude in the form of localized surface plasmons and, therefore, the spatial variation of the fields over an emitter is no longer negligible [10, 27–30]. Furthermore, the breakdown of the electric dipole selection rule leads to a multitude of "forbidden" transitions becoming accessible, which can compete with the one-photon electric dipole transition: the multipolar processes, multiquanta emission processes, and spin-flip processes [10, 15, 30].

In this article we focus on the two-photon spontaneous emission (TPSE) process that is typically 8 to 10 orders of magnitude slower than the competing spontaneous emission of a single photon [10]. Historically this second-order process in perturbation theory was predicted by Göppert-Mayer in 1931 [31]. It is the main process responsible for the mean lifetime of the 2s state of hydrogen [32], which is at the origin of the continuous spectrum coming from planetary nebulae [33]. The first estimate of this two-electric dipole transition rate was made by Breit and Teller in 1940 [32], and one decade later Spitzer and Greenstein realized a refinement and found a value of 8.23 s^{-1} [33]. It was not until 1975 that the first experimental measurement of the two-photon emission rate in hydrogen was carried out [34]. In 1981 Goldman and Drake realized the first calculations that include multipolar contributions to the TPSE process [35]. For the hydrogen atom they found that the two-magnetic dipole

* Steve.Smeets@umons.ac.be
† Bjorn.Maes@umons.ac.be
‡ Gilles.Rosolen@umons.ac.be

and the two-electric quadrupole transition rates are, respectively, 12 and 13 orders of magnitude smaller than the two-electric dipole one. More recently the TPSE process has been investigated in systems other than hydrogen, such as in quantum dots [17, 36], semiconductors [37–40], and epsilon-near-zero-materials [41].

Nowadays interest in the tailoring of this process grows [40, 42] as it has several applications [43]. For example, it promises efficient entangled photon sources for quantum applications [37, 44, 45], it allows spectroscopy to access a usually invisible part of a spectrum [44], and it leads to the conception of broadband absorbers and light emitters since this is a continuous process [46]. However, the current study of TPSE near arbitrary objects is hampered by a lack of efficient theoretical and numerical methods.

A few years ago, Muniz et al. derived an expression for the TPSE transition rate of a quantum emitter as a function of the one-photon Purcell factors, with the restriction that structures are symmetric, that the emitter is at specific positions, and under the electric dipole approximation [47]. With an analytical calculation of these factors they studied the two-photon Purcell effect near 2D plasmonic nanostructures, ideal to harness TPSE from single emitters [48].

In this paper we present an efficient and more general framework that computes the TPSE rate of a quantum emitter at any position, close to an arbitrary structure, and beyond the dipolar approximation, i.e., by taking into account the electric dipole, magnetic dipole, and electric quadrupole contributions, respectively, which is relevant for state-of-the-art current plasmonic nanostructures [10, 27–30] and for larger emitters [11–14]. Note that our framework is based on the Fermi's golden rule and is therefore limited to the weak coupling regime. Indeed, the perturbation theory is expected to fail when the ratio between the one-photon spontaneous emission rate and the transition angular frequency approaches 1 [10]. Furthermore, for the extreme cases of large emitters placed very close to a nanostructure (≈ 1 nm distance), the point approximation fails and one needs to consider the spatial extent of the emitter [14].

To this end in Section II we start with Fermi's golden rule to provide the multipolar emission channel contributions to the TPSE rate. In Section III, via the expression of the rates in terms of the dyadic Green's function, we establish for each multipolar contribution the connection between the TPSE rate and the one-photon Purcell factors. In Section IV our framework is applied to study the modification of the TPSE rate of a hydrogen-like emitter placed near a plasmonic silver nanodisk, also in an asymmetric configuration that was not handled before. The document ends with a conclusion in section V. Throughout this document we refer several times to our Supplementary Notes [49], which provide more details.

II. MULTIPOLAR EMISSION CHANNEL CONTRIBUTIONS TO THE TPSE PROCESS

In this section we discuss the contribution of the two-electric dipole, two-magnetic dipole, and two-electric quadrupole emission channels to the TPSE process. For this purpose Fermi's golden rule is reminded as it is used to calculate the transition rates, and we introduce the states involved in this second-order process. Then we present the Hamiltonian that describes the emitter-field interactions, and the electromagnetic field operators are given. Finally, we provide the multipolar emission channel contributions to the TPSE rate and describe the particular case where the environment of the emitter is vacuum.

A. Fermi's golden rule

Let us consider a system composed of a quantum emitter (e.g., an atom, a molecule, or a quantum dot) and its photonic environment. With a perturbative approach the probability per unit time that the system carries out a second-order transition by emitting two quanta from an initial state $|i\rangle$ to a final state $|f\rangle$, upon an interaction described by the Hamiltonian H_{int}, is given by Fermi's golden rule [2, 50]

$$\Gamma^{(2)}_{i\to f} = \frac{2\pi}{\hbar}\left|M^{(2)}_{fi}\right|^2 \delta(E_f - E_i) \tag{1}$$

with the second-order matrix element

$$M^{(2)}_{fi} = \sum_l \frac{\langle f|\, H_{\text{int}}\, |l\rangle \,\langle l|\, H_{\text{int}}\, |i\rangle}{E_i - E_l} \tag{2}$$

where the summation runs over all possible virtual intermediate states $|l\rangle$ of the system. In these equations $\hbar$ is the reduced Planck constant, E_a stands for the energy of the system in the state $|a\rangle$ with $a = i, l, f$, and the superscript (2) indicates that this is a second-order transition. Furthermore, this second-order transition can be seen as two successive transitions in which each one emits a quantum.

Regarding the states in this second-order process [50], the initial one is characterized by the emitter in an excited state $|e\rangle$ and the field in the vacuum state $|\text{vac}\rangle$, while in the final state the emitter is in a lower energy state $|g\rangle$ and the field is in a two-quanta state $|1_\alpha, 1_{\alpha'}\rangle$ where α and α' stand for the modes of the two emitted quanta. Thus, these two states are written as $|i\rangle = |e;\text{vac}\rangle$ and as $|f\rangle = |g; 1_\alpha, 1_{\alpha'}\rangle$, respectively. In the intermediate states that connect these two states, the emitter is in an intermediate energy state $|m\rangle$ and the field is in a one-quantum state. Depending on which mode is the first emitted quantum, the intermediate states are written as $|l\rangle = |m; 1_\alpha\rangle$ or $|l\rangle = |m; 1_{\alpha'}\rangle$. Later, the energy of the emitter in the state $|a\rangle$ will be denoted as ε_a with $a = e, m, g$.

B. Interaction Hamiltonian

When the spatial variation of the electric field at the emitter's position is not negligible, which is possible when the photonic environment is a nanostructure supporting localized surface plasmons, the standard electric dipole approximation is no longer appropriate [10, 27–30]. Therefore, we study the interaction Hamiltonian H_{int} of the system, which describes the emitter-field interactions, up to the electric quadrupolar order [6, 51]:

$$H_{\text{int}}(\mathbf{R},t) = \underbrace{-\mathbf{d}\cdot\mathbf{E}(\mathbf{R},t)}_{H_{\text{ED}}}\underbrace{-\mathbf{m}\cdot\mathbf{B}(\mathbf{R},t)}_{H_{\text{MD}}}\underbrace{-\mathbf{Q}:[\nabla\mathbf{E}(\mathbf{R},t)]}_{H_{\text{EQ}}} \tag{3}$$

in which the emitter's position $\mathbf{R}$ is taken at the center of its charge distribution. In this equation, $\nabla = (\frac{\partial}{\partial x}, \frac{\partial}{\partial y}, \frac{\partial}{\partial z})^T$ is a column vector with T denoting the transpose, the dot product is the vector scalar product, the product $\nabla\mathbf{E}$ is an outer product, whereas the double dot product is defined as $\mathbf{T}:\mathbf{U} := \sum_{i,j} T_{\ldots ij} U_{ji\ldots}$ with $\mathbf{T}$ and $\mathbf{U}$ two tensors of rank greater than or equal to two. Moreover, $\mathbf{d}$, $\mathbf{m}$, and $\mathbf{Q}$ are, respectively, the electric dipole (ED), the magnetic dipole (MD), and the electric quadrupole (EQ) moment operators.

Since a photon can be emitted by three different multipolar emission pathways (ED, MD and EQ), there are nine possible contributions to the total TPSE rate. In this paper we focus on three contributions, namely the two-electric dipole (2ED), two-magnetic dipole (2MD), and two-electric quadrupole (2EQ) second-order transitions, under which both photons are emitted by the same multipolar first-order transition. Other combinations can be derived with similar developments, but they are not relevant to the application we describe later on.

The electromagnetic field operators in equation (3) can be written as a function of the normal modes $\mathbf{A}_\alpha(\mathbf{r})$ of the vector potential [52, 53]:

$$\mathbf{E}(\mathbf{r},t) = i\sum_\alpha \sqrt{\frac{\hbar\omega_\alpha}{2\varepsilon_0}}\left\{a_\alpha(t)\mathbf{A}_\alpha(\mathbf{r}) - a_\alpha^\dagger(t)\mathbf{A}_\alpha^*(\mathbf{r})\right\}, \tag{4a}$$

$$\mathbf{B}(\mathbf{r},t) = \sum_\alpha \sqrt{\frac{\hbar}{2\varepsilon_0\omega_\alpha}}\left\{a_\alpha(t)\mathbf{B}_\alpha(\mathbf{r}) - a_\alpha^\dagger(t)\mathbf{B}_\alpha^*(\mathbf{r})\right\} \tag{4b}$$

where $\mathbf{B}_\alpha(\mathbf{r}) := \nabla\times\mathbf{A}_\alpha(\mathbf{r})$ using the vector cross product. In these equations ε_0 is the vacuum electric permittivity, whereas $a_\alpha(t)$ and $a_\alpha^\dagger(t)$ are the annihilation and creation operators of a photon in the mode α of energy $\hbar\omega_\alpha$. Note that the modes $\mathbf{A}_\alpha(\mathbf{r})$ are normalized and form a complete set of solutions of the Helmholtz equation, subject to the boundary conditions imposed by the photonic environment. These are also the conditions applied to the modes that lead to the Purcell effect.

C. Multipolar emission channel contributions to the TPSE rate

Since the states of the system and the interaction Hamiltonian are known, we can calculate each multipolar emission channel contribution to the two-photon transition rate using equations (1) to (4). If the first-order Fermi's golden rule is used instead of the second-order one, we find the three multipolar emission channel contributions to the one-photon spontaneous emission rate [50]:

$$\Gamma_{\text{ED}}^{(1)}(\mathbf{R}) = \frac{\pi}{\varepsilon_0\hbar}\sum_\alpha \omega_\alpha \left|\mathbf{d}^{eg}\cdot\mathbf{A}_\alpha\right|^2 \delta(\omega_{eg}-\omega_\alpha), \tag{5a}$$

$$\Gamma_{\text{MD}}^{(1)}(\mathbf{R}) = \frac{\pi}{\varepsilon_0\hbar}\sum_\alpha \frac{1}{\omega_\alpha} \left|\mathbf{m}^{eg}\cdot[\nabla\times\mathbf{A}_\alpha]\right|^2 \delta(\omega_{eg}-\omega_\alpha), \tag{5b}$$

$$\Gamma_{\text{EQ}}^{(1)}(\mathbf{R}) = \frac{\pi}{\varepsilon_0\hbar}\sum_\alpha \omega_\alpha \left|\mathbf{Q}^{eg}:[\nabla\mathbf{A}_\alpha]\right|^2 \delta(\omega_{eg}-\omega_\alpha) \tag{5c}$$

where the spatial dependency of the modes has been omitted. ω_α denotes the angular frequency of the photon in the mode α and $\hbar\omega_{eg} := \varepsilon_e - \varepsilon_g$ is the transition energy. Furthermore, $\mathbf{d}^{ab} := \langle a|\mathbf{d}|b\rangle$, $\mathbf{m}^{ab} := \langle a|\mathbf{d}|b\rangle$, and $\mathbf{Q}^{ab} := \langle a|\mathbf{Q}|b\rangle$ stand for the transition electric dipole, the transition magnetic dipole and the transition electric quadrupole moments, respectively, which describe the emitter's transition from the state $|b\rangle$ to the state $|a\rangle$ (a, $b = e$, m, g). Notice that the electric dipole transition is due to the field modes evaluated at the center of charge of the emitter, while the magnetic dipolar and the electric quadrupolar ones are caused by the variation of the field modes.

Now we focus on the two-photon transition rates. One shows that the two-electric dipole contribution to the TPSE rate is given by [47, 50]

$$\Gamma_{\text{2ED}}^{(2)}(\mathbf{R}) = \frac{\pi}{4\varepsilon_0^2\hbar^2}\sum_{\alpha,\alpha'}\omega_\alpha\,\omega_{\alpha'}\left|\mathbf{A}_\alpha(\mathbf{R})\cdot\boldsymbol{\mathcal{D}}^{eg}\cdot\mathbf{A}_{\alpha'}(\mathbf{R})\right|^2 \times \delta(\omega_{eg}-\omega_\alpha-\omega_{\alpha'}), \tag{6}$$

which involves a summation over the modes α and α' related to the two emitted quanta. In this equation we have defined the second rank tensor

$$\boldsymbol{\mathcal{D}}^{eg}(\omega_\alpha,\omega_{\alpha'}) := \sum_m \left(\frac{\mathbf{d}^{em}\mathbf{d}^{mg}}{\omega_{em}-\omega_\alpha} + \frac{\mathbf{d}^{mg}\mathbf{d}^{em}}{\omega_{em}-\omega_{\alpha'}}\right), \tag{7}$$

which depends on the frequencies of the two emitted quanta. The outer product is implied and $\hbar\omega_{ab} := \varepsilon_a - \varepsilon_b$. As this tensor involves two one-order transition electric dipole moments, the tensor $\boldsymbol{\mathcal{D}}^{eg}$ describes the two successive electric dipole transitions between the states $|e\rangle$ and $|g\rangle$ of the emitter. Subsequently, we refer to this tensor as the second-order transition electric dipole moment.

Following the same procedure we derive the two-magnetic dipole (2MD) and the two-electric quadrupole

(2EQ) contributions to the TPSE rate (details relative to the 2EQ contribution in the Supplementary Notes [49]):

$$\Gamma^{(2)}_{\mathrm{2MD}}(\mathbf{R}) = \frac{\pi}{4\varepsilon_0^2\hbar^2}\sum_{\alpha,\alpha'}\frac{1}{\omega_\alpha\omega_{\alpha'}}\left|[\nabla\times\mathbf{A}_\alpha]\cdot\boldsymbol{\mathcal{M}}^{eg}\cdot[\nabla\times\mathbf{A}_{\alpha'}]\right|^2 \times\delta(\omega_{eg}-\omega_\alpha-\omega_{\alpha'}), \tag{8a}$$

$$\Gamma^{(2)}_{\mathrm{2EQ}}(\mathbf{R}) = \frac{\pi}{4\varepsilon_0^2\hbar^2}\sum_{\alpha,\alpha'}\omega_\alpha\omega_{\alpha'}\left|[\nabla\mathbf{A}_\alpha]:\boldsymbol{\mathcal{Q}}^{eg}:[\nabla\mathbf{A}_{\alpha'}]\right|^2 \times\delta(\omega_{eg}-\omega_\alpha-\omega_{\alpha'}). \tag{8b}$$

In these expressions the spatial dependency of the field modes has been omitted, as well as the frequency dependency of the second rank and the fourth rank tensors defined as:

$$\boldsymbol{\mathcal{M}}^{eg}(\omega_\alpha,\omega_{\alpha'}) := \sum_m\left(\frac{\mathbf{m}^{em}\mathbf{m}^{mg}}{\omega_{em}-\omega_\alpha}+\frac{\mathbf{m}^{mg}\mathbf{m}^{em}}{\omega_{em}-\omega_{\alpha'}}\right), \tag{9a}$$

$$\boldsymbol{\mathcal{Q}}^{eg}(\omega_\alpha,\omega_{\alpha'}) := \sum_m\left(\frac{\mathbf{Q}^{em}\,\mathbf{Q}^{mg}}{\omega_{em}-\omega_\alpha}+\frac{\mathbf{Q}^{mg}\,\mathbf{Q}^{em}}{\omega_{em}-\omega_{\alpha'}}\right) \tag{9b}$$

where the outer product is implied. The components of the tensor that derive from the outer product of two tensors $\mathbf{U}$ and $\mathbf{V}$ are $(\mathbf{UV})_{i_1,i_2,\ldots,i_n,j_1,j_2,\ldots,j_n} := U_{i_1,i_2,\ldots,i_n}V_{j_1,j_2,\ldots,j_n}$. Thus, these tensors describe the two successive magnetic dipole and electric quadrupole transitions, respectively, between the states $|e\rangle$ and $|g\rangle$ of the emitter. Subsequently, we refer to them as the second-order transition magnetic dipole and electric quadrupole moments. Note that since $\mathbf{Q}$ is symmetric, the fourth rank tensor $\boldsymbol{\mathcal{Q}}^{eg}$ is also symmetric (i.e., $\forall i,j,k,l = 1,2,3$, $\mathcal{Q}^{eg}_{ijkl} = \mathcal{Q}^{eg}_{jikl}$ and $\mathcal{Q}^{eg}_{ijkl} = \mathcal{Q}^{eg}_{ijlk}$). Moreover, since $\mathbf{Q}$ can be taken traceless [54, 55], with the definition of $\boldsymbol{\mathcal{Q}}^{eg}$, the tensor satisfies the two following properties: $\forall k,l = 1,2,3$, $\sum_{i=1}^3\mathcal{Q}^{eg}_{iikl} = 0$ and $\forall i,j = 1,2,3$, $\sum_{k=1}^3\mathcal{Q}^{eg}_{ijkk} = 0$.

The derived equations (6) and (8) for the multipolar contributions to the TPSE rate are valid regardless of the emitter environment. We will now derive the rate of these transitions in vacuum. The obtained expressions will be useful in section III to normalize transition rates, and to derive expressions for the multipolar contributions that can be computed through classical electromagnetic simulations.

D. Free-space TPSE rate

In free-space the field modes are plane waves defined by a wave vector $\mathbf{k}$ and a unitary polarization vector $\boldsymbol{\varepsilon}_{\mathbf{k},s}$ where the parameter $s = 1,2$ represents the two transverse polarizations [50, 52]. Consequently, the field modes in equations (6) and (8) become

$$\mathbf{A}_\alpha(\mathbf{r}) \longrightarrow \mathbf{A}_{\mathbf{k},s}(\mathbf{r}) = \frac{e^{i\mathbf{k}\cdot\mathbf{r}}}{\sqrt{V}}\boldsymbol{\varepsilon}_{\mathbf{k},s} \tag{10}$$

where V stands for the arbitrary and finite box quantization volume in which the field is assumed to be confined. In this case the summation over the modes α becomes [50, 52]

$$\sum_\alpha \longrightarrow \sum_{s=1}^2\sum_{\mathbf{k}} \overset{V\to\infty}{\longrightarrow} \frac{V}{(2\pi)^3}\sum_{s=1}^2\int \mathrm{d}^3k. \tag{11}$$

The calculations for the 2ED transition can be found in [50], while the calculations relative to the 2EQ transition is in our Supplementary Notes [49]. Thus, for each multipolar operator MO $\in$ {ED, MD, EQ} the free-space TPSE rate is given by

$$\Gamma^{(2)}_{\mathrm{2MO},0} = \int_0^{\omega_{eg}}\gamma^{(2)}_{\mathrm{2MO},0}(\omega)\,\mathrm{d}\omega \tag{12}$$

where each multipolar contribution $\gamma^{(2)}_{\mathrm{2MO},0}(\omega)$ to the spectral distribution of the emitted quanta $\gamma^{(2)}_0(\omega)$ is given by

$$\gamma^{(2)}_{\mathrm{2ED},0}(\omega) = \frac{\omega^3(\omega_{eg}-\omega)^3}{36\pi^3\varepsilon_0^2\hbar^2c^6}\left\|\boldsymbol{\mathcal{D}}^{eg}(\omega,\omega_{eg}-\omega)\right\|^2, \tag{13a}$$

$$\gamma^{(2)}_{\mathrm{2MD},0}(\omega) = \frac{\omega^3(\omega_{eg}-\omega)^3}{36\pi^3\varepsilon_0^2\hbar^2c^{10}}\left\|\boldsymbol{\mathcal{M}}^{eg}(\omega,\omega_{eg}-\omega)\right\|^2, \tag{13b}$$

$$\gamma^{(2)}_{\mathrm{2EQ},0}(\omega) = \frac{\omega^5(\omega_{eg}-\omega)^5}{400\pi^3\varepsilon_0^2\hbar^2c^{10}}\left\|\boldsymbol{\mathcal{Q}}^{eg}(\omega,\omega_{eg}-\omega)\right\|^2, \tag{13c}$$

where c denotes the speed of light in vacuum, and the squared norm of an n^{th} rank tensor $\mathbf{U}$ with $n\in\mathbb{N}_0$ is $\|\mathbf{U}\|^2 := \sum_{i_1,i_2,\ldots,i_n}|U_{i_1,i_2,\ldots,i_n}|^2$.

III. RELATION BETWEEN THE TPSE RATE AND PURCELL FACTORS

A connection between the TPSE rate of an emitter and the Purcell factors related to the one-photon spontaneous emission (OPSE) process was established for the 2ED transition [47]. However, this formula can only be used in the basis that diagonalizes the imaginary part of the dyadic Green's function independently of the frequency, which is a condition that only allows the study of symmetric structures with emitters at specific positions. In further work, this formula was used to calculate TPSE spectra for the 2ED transition of a hydrogen-like emitter placed under a plasmonic two-dimensional silver nanodisk [48]. However, because of the aforementioned condition on the basis, they could only study the case where the emitter is on the axis of symmetry of the disk.

Consequently, it is interesting to take into account corrective terms, linked to the off-diagonal components of the imaginary part of the Green's function, in order to derive general formulas for the 2ED, 2MD and 2EQ transition rates, which can be used for structures of arbitrary shape and at any emitter's position. Moreover, since the derived formulas are based on the calculation of Purcell factors, we emphasize here that the TPSE rate of an

emitter can be determined through conventional classical electromagnetic simulations, thus allowing to consider arbitrary shaped nanostructures.

To this end we first normalize the multipolar contributions to the TPSE rate, equations (6) and (8), with the free-space rates, and rewrite them as a function of the dyadic Green's function $\mathbf{G}$. Its imaginary part admits a spectral representation that can be expanded in terms of the normal modes $\mathbf{A}_\alpha$ of the electromagnetic field [6]:

$$\mathrm{Im}\mathbf{G}(\omega;\mathbf{r},\mathbf{r}') = \frac{\pi c^2}{2\omega}\sum_\alpha \mathbf{A}_\alpha(\mathbf{r})\mathbf{A}_\alpha^*(\mathbf{r}')\,\delta(\omega-\omega_\alpha). \quad (14)$$

Then, for each multipolar contribution we establish a connection between the Green's function and the one-photon Purcell factors. We start with the 2ED transition, next we extend this relation for the 2MD transition, and lastly for the 2EQ transition (detailed derivation in Supplementary Notes [49]).

A. Two-electric dipole transitions

By involving the Green's function and dividing the obtained spectral density $\gamma^{(2)}_{\mathrm{2ED}}(\omega;\mathbf{R})$ by the free-space one (equation (13a)) we obtain [47]:

$$\begin{aligned}\frac{\gamma^{(2)}_{\mathrm{2ED}}(\omega;\mathbf{R})}{\gamma^{(2)}_{\mathrm{2ED},0}(\omega)} =& \hat{\mathcal{D}}^{eg}_{ia}(\omega,\omega_{eg}-\omega)\left(\hat{\mathcal{D}}^{eg}_{jb}(\omega,\omega_{eg}-\omega)\right)^* \\ &\times \frac{6\pi c}{\omega}\,\mathrm{Im}G_{ij}(\omega;\mathbf{R},\mathbf{R}) \\ &\times \frac{6\pi c}{\omega_{eg}-\omega}\,\mathrm{Im}G_{ab}(\omega_{eg}-\omega;\mathbf{R},\mathbf{R}) \quad (15)\end{aligned}$$

where the Einstein summation convention is used and the caret denotes normalized tensors (i.e., for an n^{th} rank tensor $\mathbf{U}$ with $n\in\mathbb{N}_0$, $\hat{\mathbf{U}} := \mathbf{U}/\|\mathbf{U}\|$). Note that the indices i and j are related to the quantum emitted at the frequency ω while the indices a and b concern the quantum emitted at the complementary frequency $\omega_{eg}-\omega$.

Relation with the Purcell factors

In order to establish the relation between the components of the Green's function and the one-photon Purcell factors, let us consider the ED transition rate written as [6]:

$$\frac{\Gamma^{(1)}_{\mathrm{ED}}(\mathbf{R})}{\Gamma^{(1)}_{\mathrm{ED},0}} = \hat{d}^{eg}_i\left(\hat{d}^{eg}_j\right)^*\frac{6\pi c}{\omega_{eg}}\,\mathrm{Im}G_{ij}(\omega_{eg};\mathbf{R},\mathbf{R}) \quad (16)$$

where $\hat{\mathbf{d}}^{eg}$ stands for the normalized one-order transition electric dipole moment.

A general electric dipole moment can be expanded with an orthonormal basis of three dipoles. We define the Purcell factors P_i^{ED}, which correspond to the ratio between the ED transition rate of an emitter that has its transition electric dipole moment aligned along one of the basis vectors (i.e., $\hat{\mathbf{d}}^{eg} := \hat{\mathbf{e}}_i$ with $i=1,2,3$) and the corresponding rate in free space as [47]:

$$P_i^{\mathrm{ED}}(\omega;\mathbf{R}) := \frac{6\pi c}{\omega}\mathrm{Im}G_{ii}(\omega;\mathbf{R},\mathbf{R}). \quad (17)$$

Furthermore, we define the Purcell factors P_{ij}^{ED} relative to an emitter that has its transition electric dipole moment aligned along the bisector of two basis vectors (i.e., $\hat{\mathbf{d}}^{eg} := (\hat{\mathbf{e}}_i+\hat{\mathbf{e}}_j)/\sqrt{2}$ with $i,j=1,2,3$ and $i\neq j$) as

$$\begin{aligned}P_{ij}^{\mathrm{ED}}(\omega;\mathbf{R}) :=& \frac{1}{2}\left(P_i^{\mathrm{ED}}(\omega;\mathbf{R})+P_j^{\mathrm{ED}}(\omega;\mathbf{R})\right) \\ &+\frac{6\pi c}{\omega}\mathrm{Im}G_{ij}(\omega;\mathbf{R},\mathbf{R}) \quad (18)\end{aligned}$$

where we used the definition of the Purcell factors P_i^{ED} as well as the symmetry property of the tensor $\mathrm{Im}\mathbf{G}$ [56].

We can now rewrite equation (15) as

$$\begin{aligned}\frac{\gamma^{(2)}_{\mathrm{2ED}}(\omega;\mathbf{R})}{\gamma^{(2)}_{\mathrm{2ED},0}(\omega)} =& \hat{\mathcal{D}}^{eg}_{ia}(\omega,\omega_{eg}-\omega)\left(\hat{\mathcal{D}}^{eg}_{jb}(\omega,\omega_{eg}-\omega)\right)^* \\ &\times F^{ED}_{ij}(\omega;\mathbf{R})\,F^{ED}_{ab}(\omega_{eg}-\omega;\mathbf{R}) \quad (19)\end{aligned}$$

where the components of the tensor $\mathbf{F}^{\mathrm{ED}}$ are defined as

$$F^{\mathrm{ED}}_{ii}(\omega;\mathbf{R}) := \frac{6\pi c}{\omega}\mathrm{Im}G_{ii}(\omega;\mathbf{R},\mathbf{R}) = P_i^{\mathrm{ED}}(\omega;\mathbf{R}), \quad (20)$$

$$\begin{aligned}F^{\mathrm{ED}}_{ij}(\omega;\mathbf{R}) :=& \frac{6\pi c}{\omega}\mathrm{Im}G_{ij}(\omega;\mathbf{R},\mathbf{R}) \\ =& P_{ij}^{\mathrm{ED}}(\omega;\mathbf{R}) - \frac{1}{2}\left(P_i^{\mathrm{ED}}(\omega;\mathbf{R})+P_j^{\mathrm{ED}}(\omega;\mathbf{R})\right) \quad (21)\end{aligned}$$

with $i,j=1,2,3$ and $i\neq j$. Note that we can also rewrite equation (16) of the ED transition rate as a function of this tensor.

Since this tensor $\mathbf{F}^{\mathrm{ED}}$ is also symmetric we need to calculate in the most general case six Purcell factors to get the 2ED transition rate. For example, in a cartesian basis we need to calculate these six factors:

$$\left\{P_x^{\mathrm{ED}},P_y^{\mathrm{ED}},P_z^{\mathrm{ED}},P_{yz}^{\mathrm{ED}},P_{xz}^{\mathrm{ED}},P_{xy}^{\mathrm{ED}}\right\}. \quad (22)$$

In free-space all Purcell factors are equal to one and so the tensor $\mathbf{F}^{\mathrm{ED}}$ is equal to the identity matrix.

As a consistency check, in the basis that diagonalizes the imaginary part of the Green's function simultaneously at the frequencies of the two emitted quanta (or in the range of the studied spectrum), we retrieve the less general formula (valid only in this specific basis) that involves only the three Purcell factors P_i^{ED} [47]:

$$\begin{aligned}\frac{\gamma^{(2)}_{\mathrm{2ED}}(\omega;\mathbf{R})}{\gamma^{(2)}_{\mathrm{2ED},0}(\omega)} =& \left|\hat{\mathcal{D}}^{eg}_{ia}(\omega,\omega_{eg}-\omega)\right|^2 \\ &\times P_i^{ED}(\omega;\mathbf{R})\,P_a^{ED}(\omega_{eg}-\omega;\mathbf{R}). \quad (23)\end{aligned}$$

B. Two-magnetic dipole transition

Similar developments lead to the 2MD transition rate:

$$\frac{\gamma^{(2)}_{\mathrm{2MD}}(\omega;\mathbf{R})}{\gamma^{(2)}_{\mathrm{2ED},0}(\omega)} = \hat{\mathcal{M}}^{eg}_{ia}(\omega,\omega_{eg}-\omega)\left(\hat{\mathcal{M}}^{eg}_{jb}(\omega,\omega_{eg}-\omega)\right)^{*} \times F^{\mathrm{MD}}_{ij}(\omega;\mathbf{R})\,F^{\mathrm{MD}}_{ab}(\omega_{eg}-\omega;\mathbf{R}) \quad (24)$$

involving the normalized second-order transition magnetic dipole moment, as well as the tensor $\mathbf{F}^{\mathrm{MD}}$. The equations (20) and (21) that establish the link between the tensor $\mathbf{F}^{\mathrm{ED}}$ and the Purcell factors for the ED transition are also valid for the MD transition, where the Purcell factors are defined in the same way, but with the transition magnetic dipole moment instead.

C. Two-electric quadrupole transition

Let us now focus on the 2EQ transition. Via the Green's function (equation (14)) and dividing the obtained spectral density $\gamma^{(2)}_{\mathrm{2EQ}}(\omega;\mathbf{R})$ by the free-space one (equation (13c)) we get [49]:

$$\frac{\gamma^{(2)}_{\mathrm{2EQ}}(\omega;\mathbf{R})}{\gamma^{(2)}_{\mathrm{2EQ},0}(\omega)} = \hat{\mathcal{Q}}^{eg}_{ijab}(\omega,\omega_{eg}-\omega)\left(\hat{\mathcal{Q}}^{eg}_{klcd}(\omega,\omega_{eg}-\omega)\right)^{*} \times T_{ijkl}(\omega;\mathbf{R})\,T_{abcd}(\omega_{eg}-\omega;\mathbf{R}) \quad (25)$$

where the Einstein summation convention is used and $\hat{\boldsymbol{\mathcal{Q}}}^{eg}$ stands for the normalized second-order transition electric quadrupole moment. Note that the indices i,j,k and l are related to the quanta emitted at the frequency ω, while the indices a,b,c and d concern the quanta emitted at the complementary frequency $\omega_{eg}-\omega$.

In the previous equation we use the fourth rank tensor $\mathbf{T}$ defined as:

$$T_{ijkl}(\omega;\mathbf{R}) := \frac{20\pi c^3}{\omega^3}\left\{\partial_j\partial_{l'}\mathrm{Im}G_{ik}(\omega;\mathbf{r},\mathbf{r}')\right\}_{\mathbf{r}=\mathbf{r}'=\mathbf{R}} \quad (26)$$

where ∂_j and $\partial_{l'}$ mean derivatives with respect to, respectively, the coordinates $\mathbf{r}$ and $\mathbf{r}'$. Since $\mathbf{T}$ is a real tensor, by using equation (14) we can show that it satisfies the property: $\forall i,j,k,l=1,2,3,\ T_{ijkl}=T_{klij}$.

The derived equation contains 9^4 terms. Fortunately, we can use the property of the tensor $\mathbf{T}$ mentioned above, as well as the properties of the tensor $\boldsymbol{\mathcal{Q}}^{eg}$ derived from the symmetric and traceless properties of electric quadrupole moments (cf. Section II C), to remove redundant components. We obtain a formula involving only $(\sum_{n=1}^{5} n)^2 = 15^2$ terms [49]:

$$\frac{\gamma^{(2)}_{\mathrm{2EQ}}(\omega;\mathbf{R})}{\gamma^{(2)}_{\mathrm{2EQ},0}(\omega)} = \sum_{\substack{\mu,\nu=1\\ \nu\geq\mu}}^{5}\sum_{\substack{\alpha,\beta=1\\ \beta\geq\alpha}}^{5} \hat{\mathcal{Q}}^{eg}_{\mu\alpha\nu\beta}(\omega,\omega_{eg}-\omega) \times F^{\mathrm{EQ}}_{\mu\nu}(\omega;\mathbf{R})\,F^{\mathrm{EQ}}_{\alpha\beta}(\omega_{eg}-\omega;\mathbf{R}) \quad (27)$$

where the indices μ and ν are relative to the first quantum, while the indices α and β are relative to the second one. In this equation the second rank tensor $\mathbf{F}^{\mathrm{EQ}}$ in five dimensions is expressed as a function of the tensor $\mathbf{T}$ [49], and the components of the fourth rank tensor $\hat{\boldsymbol{\mathcal{Q}}}^{eg}$ in five dimensions is defined as:

$$\hat{\mathcal{Q}}_{\mu\alpha\nu\beta} := \begin{cases} \hat{\mathcal{Q}}_{\mu\alpha}\hat{\mathcal{Q}}^{*}_{\nu\beta} & \forall \mu=\nu,\ \alpha=\beta \\ \hat{\mathcal{Q}}_{\mu\alpha}\hat{\mathcal{Q}}^{*}_{\nu\beta}+\hat{\mathcal{Q}}_{\mu\beta}\hat{\mathcal{Q}}^{*}_{\nu\alpha} & \forall \mu=\nu,\ \alpha<\beta \\ \hat{\mathcal{Q}}_{\mu\alpha}\hat{\mathcal{Q}}^{*}_{\nu\beta}+\hat{\mathcal{Q}}_{\nu\alpha}\hat{\mathcal{Q}}^{*}_{\mu\beta} & \forall \mu<\nu,\ \alpha=\beta \\ 2\hat{\mathcal{Q}}_{\mu\alpha}\hat{\mathcal{Q}}^{*}_{\nu\beta}+2\hat{\mathcal{Q}}_{\mu\beta}\hat{\mathcal{Q}}^{*}_{\nu\alpha} & \forall \mu<\nu,\ \alpha<\beta \end{cases} \quad (28)$$

where the eg superscript and the dependencies are omitted.

To derive this formula we use a modified version of the Voigt notation. This mathematical convention exploits the symmetry and the traceless properties of a tensor, by removing its redundant components, to represent it by a lower rank tensor defined in a higher dimensional space. In this way the one-order and two-order transition electric quadrupole moments, which are second rank and fourth rank tensors in three dimensions, are represented by means of a vector and a second rank tensor in five dimensions, respectively. Table I establishes the correspondence between the new indices and these of the represented tensors.

(i,j)	$(1,1)$	$(2,2)$	$(2,3)$	$(1,3)$	$(1,2)$
μ	1	2	3	4	5

TABLE I. Modified Voigt notation: correspondence between the pair of indices (i,j) of a symmetric and traceless tensor in three dimensions and the indices μ in five dimensions. The indices $\mu=1,2$ correspond to the two independent diagonal components of a second rank tensor, while the indices $\mu=3,4,5$ correspond to its three independent off-diagonal components. By convention, the indices of this notation are denoted with Greek letters.

Relation with the Purcell factors

As for the 2ED transition we first consider the one-photon EQ transition rate in order to establish the relation between the tensor $\mathbf{F}^{\mathrm{EQ}}$ and the one-photon Purcell factors, which are defined here as the ratio between the one-photon EQ transition rate and the corresponding rate in free-space.

We can show that the EQ transition can be written as [49]:

$$\frac{\Gamma^{(1)}_{\mathrm{EQ}}(\mathbf{R})}{\Gamma^{(1)}_{\mathrm{EQ},0}} = \sum_{\substack{\mu,\nu=1\\ \nu\geq\mu}}^{5} \hat{Q}^{eg}_{\mu\nu}\,F^{\mathrm{EQ}}_{\mu\nu}(\omega_{eg};\mathbf{R}) \quad (29)$$

with the second rank tensor $\hat{\mathbf{Q}}^{eg}$ in five dimensions de-

fined as

$$\hat{Q}^{eg}_{\mu\nu} := \begin{cases} \hat{Q}^{eg}_{\mu}(\hat{Q}^{eg}_{\mu})^* & \forall \mu = \nu \\ 2\hat{Q}^{eg}_{\mu}(\hat{Q}^{eg}_{\nu})^* & \forall \mu < \nu. \end{cases} \tag{30}$$

Since a general electric quadrupole moment involves up to five independent components, it can be expanded with a basis of 5 quadrupoles. To construct this basis we consider two different types of quadrupole, sketched in Figure 1. In our notation these quadrupoles are represented by a vector in five dimensions where only the μ-th component is non-zero and equals to $1/\sqrt{2}$.

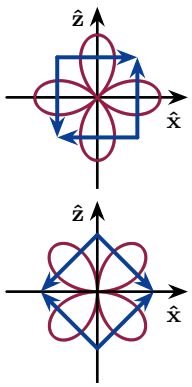

Type I

$$\hat{\mathbf{Q}}_{xz} = \tfrac{1}{\sqrt{2}} \begin{pmatrix} 0 & 0 & 1 \\ 0 & 0 & 0 \\ 1 & 0 & 0 \end{pmatrix} = \left(0, 0, 0, 1/\sqrt{2}, 0\right)^T$$

Type II

$$\hat{\mathbf{Q}}_{xx} = \tfrac{1}{\sqrt{2}} \begin{pmatrix} 1 & 0 & 0 \\ 0 & 0 & 0 \\ 0 & 0 & -1 \end{pmatrix} = \left(1/\sqrt{2}, 0, 0, 0, 0\right)^T$$

FIG. 1. Representation of the two considered types of plane quadrupole configurations. Type II differs from type I by a rotation of 45° in the plane and involves only diagonal components, while type I involves solely off-diagonal components. They are represented by means of four dipoles of same norm (blue arrows) and the radiation patterns are sketched in dark red. The modified Voigt notation is used to represent their tensor by the means of a five-dimensional vector.

First, we define five Purcell factors P^{EQ}_{μ} where the indices $\{\mu = 1, \ldots, 5\}$ correspond, respectively, to the indices $\{xx, yy, yz, xz, xy\}$ (three types I and two types II[1]):

$$P^{\mathrm{EQ}}_{\mu}(\omega; \mathbf{R}) := \frac{1}{2} F^{\mathrm{EQ}}_{\mu\mu}(\omega; \mathbf{R}) \qquad \forall \mu = 1, \ldots, 5. \tag{31}$$

These factors correspond to the ratio between the EQ transition rate of an emitter for which its transition electric quadrupole moment is the basis tensor $\hat{\mathbf{Q}}_{\mu}$ and the corresponding rate in free space.

Second, we consider all of the possible combinations of the basis quadrupoles[2]:

$$\hat{\mathbf{Q}}_{\mu\nu} := \frac{1}{N}\left(\hat{\mathbf{Q}}_{\mu} + \hat{\mathbf{Q}}_{\nu}\right) \qquad \forall \mu, \nu = 1, \ldots, 5 \; ; \; \mu < \nu \tag{32}$$

with N a normalization constant. This allows us to define ten Purcell factors:

$$P^{\mathrm{EQ}}_{\mu\nu} := \begin{cases} \frac{1}{3}\left(P_{\mu} + P_{\nu} + F_{\mu\nu}\right) & \text{if } (\mu, \nu) = (1, 2) \\ \frac{1}{2}\left(P_{\mu} + P_{\nu} + F_{\mu\nu}\right) & \forall \mu, \nu = 2, 3, 4, 5 \; ; \; \mu < \nu \end{cases} \tag{33}$$

where the EQ superscript and the dependencies have been omitted and where the Purcell factors $P^{\mathrm{EQ}}_{\mu\nu}$ are relative to an emitter that has its transition electric quadrupole moment described by the tensor $\hat{\mathbf{Q}}_{\mu\nu}$ (i.e., an equal and linear combination of the tensors $\hat{\mathbf{Q}}_{\mu}$ and $\hat{\mathbf{Q}}_{\nu}$).

To summarize, we established a relation between the 15 independent components of the symmetric tensor $\mathbf{F}^{\mathrm{EQ}}$, which are related to the derivatives of the imaginary part of the dyadic Green's function, and 15 Purcell factors:

$$F^{\mathrm{EQ}}_{\mu\nu}(\omega; \mathbf{R}) = \begin{cases} 2P^{\mathrm{EQ}}_{\mu} & \forall \mu = \nu \\ 3P^{\mathrm{EQ}}_{\mu\nu} - P^{\mathrm{EQ}}_{\mu} - P^{\mathrm{EQ}}_{\nu} & \text{if } (\mu, \nu) = (1, 2) \\ 2P^{\mathrm{EQ}}_{\mu\nu} - P^{\mathrm{EQ}}_{\mu} - P^{\mathrm{EQ}}_{\nu} & \text{else} \end{cases} \tag{34}$$

where the dependencies have been omitted. Thus, in the most general case these 15 Purcell factors are necessary to calculate the 2EQ transition rate:

$$\left\{P^{\mathrm{EQ}}_{\mu}\right\} \cup \left\{P^{\mathrm{EQ}}_{\mu\nu}\right\} \tag{35}$$

where the indices $\mu, \nu = 1, \ldots, 5$ with $\mu < \nu$ correspond to the indices $\{xx, yy, yz, xz, xy\}$. In vacuum all Purcell factors tend towards one and so $\mathbf{F}^{\mathrm{EQ}}$ is given by

$$F^{\mathrm{EQ}}_{\mu\nu} = \begin{cases} 2 & \forall \mu = \nu \\ 1 & \text{if } (\mu, \nu) = (1, 2) \\ 0 & \text{else.} \end{cases} \tag{36}$$

D. Discussion

It is important to note that the derived equations for the multipolar contributions to the total TPSE rate (equations (19), (24), and (27)) are valid regardless of the emitter environment. It is thus possible to calculate the change in spontaneous emission rates when the emitter is placed in a given photonic environment. Moreover, the contribution of the electronic structure of the emitter and the contribution of the photonic environment are decoupled in these equations, and thus can be calculated separately. Indeed, each equation involves two tensors. The first one is the normalized multipolar second-order transition moment that depends only on the electronic structure. The second one is the tensor $\mathbf{F}^{\mathrm{MO}}$, with MO $\in$ {ED, MD, EQ}, presents for the two emitted quanta of complementary energy and that is expressed as a function of the one-photon Purcell factors, and thus it depends only on the photonic environment.

[1] We do not need to consider the type II quadrupole $\hat{\mathbf{Q}}_{zz}$ because in our modified Voigt notation, we removed the last diagonal component to remove redundancy with respect to the traceless property.

[2] Note that all considered quadrupoles need to be normalized and that the quadrupole $\hat{\mathbf{Q}}_{xxyy} = (\hat{\mathbf{Q}}_{xx} + \hat{\mathbf{Q}}_{yy})/\sqrt{3}$ is the linear quadrupole represented by the diagonal matrix $1/\sqrt{6}\,\mathrm{diag}(1, 1, -2)$.

It is known that the Purcell factors can be computed classically by the ratio of the power emitted by a classical emitter (i.e., a radiating point ED, MD, or EQ) in presence of the photonic environment and in free-space $P^{\mathrm{MO}}(\omega;\mathbf{R}) = W_{\mathrm{MO}}(\omega;\mathbf{R})/W_{\mathrm{MO},0}(\omega)$ [6]. Furthermore, there is a dependency on the emitter's orientation with respect to the photonic environment. In the end these Purcell factors can be computed by modelling point sources in conventional electromagnetic software packages (with e.g., Finite Element Method [57], Finite-Difference Time-Domain Method [58], etc.). The expression of the free-space emitted power for point sources can be found in [54].

In an emission process a quantum can be emitted either radiatively in case of photon emission to the far field, or non-radiatively in case of energy absorption by the environment. Since our framework is based on Purcell factors we can separate the contributions of the radiative and non-radiative emission channels to the TPSE process [48]. They can be calculated through the decomposition into radiative and non-radiative parts of the total Purcell factors: $P^{\mathrm{MO}}(\omega,\mathbf{r}) = P^{\mathrm{MO}}_{\mathrm{r}}(\omega,\mathbf{r}) + P^{\mathrm{MO}}_{\mathrm{nr}}(\omega,\mathbf{r})$ [6, 48].

Furthermore, as the TPSE process is continuous [59], retrieving a full TPSE spectrum requires the calculation of the Purcell factors over a range of frequencies. In addition, at each frequency the Purcell factors need to be calculated for different source orientations. In the most general case, 6 Purcell factors are needed for the dipolar transitions (cf. equation (22)), while for the quadrupolar one 15 are needed (cf. equation (35)). However, depending on the symmetry of the studied photonic environment some factors can be equal, thus reducing the number of Purcell factors to calculate.

Once the one-photon Purcell factors are calculated classically, one can straightforwardly determine each multipolar contribution to the TPSE rate via equations (19), (24), and (27) when the normalized multipolar second-order transition moments are known. In our framework these are calculated analytically via the wave functions of the emitter.

IV. APPLICATION

As a validation step of the developed framework, we study the two-photon Purcell effect for an $s \to s$ transition of a hydrogen atom placed 10 nm under a quasi-two-dimensional silver nanodisk, with the same system's parameters as in [48]. In this study, they calculated the 2ED contribution to the TPSE rate in the specific case where the emitter is placed on the axis of symmetry of the disk and with an analytical calculation of Purcell factors [48]. With our more general framework, the Purcell factors are computed numerically and the 2EQ contribution is also determined. Subsequently, we exploit the flexibility of our method in the case of an off-axis emitter. Note that since the considered structure is not relevant to enhance MD transitions [22], we did not calculate the magnetic contributions to the TPSE rate. Furthermore, the mixed ED-EQ two-photon $s \to s$ transition is not allowed by selection rules [35, 60]. Our methods are explained below and then the results are presented and discussed.

A. Methods

Concerning the analytical calculation of the second-order transition moments, the determination of the tensor $\boldsymbol{\mathcal{D}}^{eg}$ can be found in [47] while the derivation of $\boldsymbol{\mathcal{Q}}^{eg}$ is given in our Supplementary Notes [49]. The obtained tensors are independent of the frequencies of the emitted quanta and are respectively given by

$$\hat{\boldsymbol{\mathcal{D}}}^{eg} = \frac{\mathbb{1}_3}{\sqrt{3}}, \tag{37a}$$

$$\hat{\boldsymbol{\mathcal{Q}}}^{eg} = \frac{1}{\sqrt{20}} \begin{pmatrix} 4/3 & -2/3 & 0 & 0 & 0 \\ -2/3 & 4/3 & 0 & 0 & 0 \\ 0 & 0 & 1 & 0 & 0 \\ 0 & 0 & 0 & 1 & 0 \\ 0 & 0 & 0 & 0 & 1 \end{pmatrix} \tag{37b}$$

where $\mathbb{1}_3$ is the identity matrix in three dimensions.

Near a low-loss plasmonic structure the non-radiative emission channel is dominated by the excitation of dark plasmonic modes, leading to absorption and no emission in the far field [48]. Thus, the two-quanta spontaneous emission process of an emitter close to this type of structure is dominated by three emission pathways, namely the photon-photon, photon-plasmon, and plasmon-plasmon channels (Figure 2), which can be computed through the decomposition of the Purcell factors into radiative and non-radiative parts.

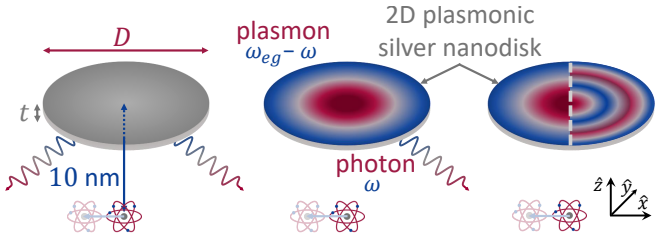

FIG. 2. From left to right: photon-photon, photon-plasmon, and plasmon-plasmon emission channels of the TPSE rate between two symmetric states of a quantum emitter. The latter is placed on-axis or off-axis 10 nm below a 5.2 Å thickness silver disk and its transition frequency is $\hbar\omega_{eg} = 2.64$ eV, which corresponds to a wavelength of 470 nm. The first quantum is emitted at the frequency ω while the second one is emitted at the complementary frequency $\omega_{eg} - \omega$.

When the emitter is on-axis the system has azimuthal symmetry, reducing the number of Purcell factors to calculate. Thus, at each frequency three Purcell factors for the dipolar transition and seven for the quadrupolar one need to be calculated: $\left\{P_x^{\mathrm{ED}}, P_z^{\mathrm{ED}}, P_{xz}^{\mathrm{ED}}\right\}$ and

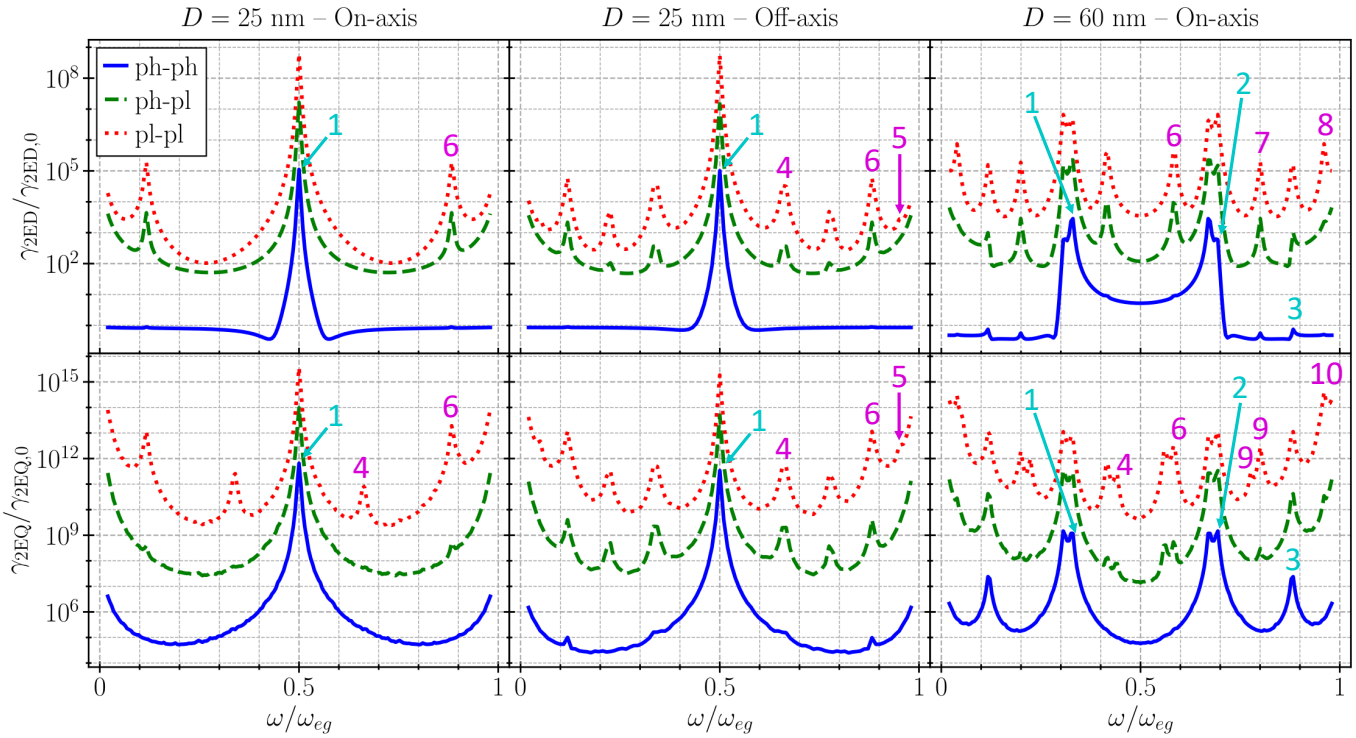

FIG. 3. Photon-photon (ph-ph), photon-plasmon (ph-pl), and plasmon-plasmon (pl-pl) relaxation channels of the spectral TPSE rate for the 2ED (top row) and 2EQ (bottom row) transitions between two symmetric states of a quantum emitter. The latter is placed 10 nm below a 5.2 Å thickness silver disk and its transition frequency is $\hbar\omega_{eg} = 2.64$ eV. The first two columns correspond to a 25 nm diameter disk, while for the third one the diameter is 60 nm. The emitter is placed on the axis of symmetry of the disk, except for the central column where it is shifted in the direction parallel to the disk by $D/4$. The spectra were computed over 199 frequencies for the emitter on-axis and over 99 frequencies for the emitter off-axis. The first quantum is emitted at the frequency ω while the second one is emitted at the complementary frequency $\omega_{eg} - \omega$, leading to symmetric spectra. In Figure 4, the surface current density on the disk corresponding to some radiative and non-radiative peaks, which are identified by respectively a cyan and magenta number, is plotted.

$\{P^{\rm EQ}_{xx}, P^{\rm EQ}_{xz}, P^{\rm EQ}_{xy}, P^{\rm EQ}_{xxyy}, P^{\rm EQ}_{xxxz}, P^{\rm EQ}_{xxxy}, P^{\rm EQ}_{xzxy}\}$, where the Z direction has been taken perpendicular to the disk. In contrast, when the emitter is shifted in the X direction, the system has no longer an azimuthal symmetry but rather a XZ-plane mirror symmetry and all factors (6+15) need to be calculated (cf. equations (22) and (35)).

In practice each Purcell factor is computed over a range of frequencies with the COMSOL Multiphysics® software, which is based on the Finite Element Method, on a single core of a computer using an AMD Ryzen Threadripper PRO 5995WX CPU and 256GB of RAM, thus enabling parallel computation. The parameters of our COMSOL models in the frequency domain are the following. First, the domain is a sphere with a radius equal to the studied wavelength λ and an unstructured tetrahedral mesh is used where the smallest element has a characteristic size of 0.25 nm. Second, Perfectly Matched Layers (PMLs) are defined as an outer layer of the domain with a thickness of $\lambda/4$. Third, the silver nanodisk is modelled using a cylinder with a height $t = 5.2$ Å and a diameter $D = 25$ or 60 nm. Its optical response is given by the Drude conductivity $\sigma(\omega) = \varepsilon_0\tau\omega_p^2/(1 - i\omega\tau)$ with the plasma frequency $\hbar\omega_p = 9.1$ eV and the relaxation rate of silver $\hbar\tau^{-1} = 18$ meV, as used in [48]. Fourth, the classical emitter is placed 10 nm under the nanodisk and is modelled by a radiating electric point dipole or quadrupole. Fifth, the Purcell factors are calculated by integration of the emitted power either at the inner surface of the PML for the radiative part or at the surface of a fictional sphere of 5 nm radius centered on the emitter for the total part (radiative plus non-radiative).

B. Results

The photon-photon, photon-plasmon, and plasmon-plasmon relaxation channels of the spectral TPSE rate for the 2ED and 2EQ contributions are plotted in Figure 3. The emitter is placed on-axis for the spectra in the first and in the last columns, while it is shifted by a quantity $D/4$ in the plane parallel to the disk for the spectra in the central column. The computation of one Purcell factor over 199 frequencies has required 45 minutes and 13 GB of RAM for the 25 nm diameter disk, and 135 minutes and 30 GB of RAM for the 60 nm diameter one.

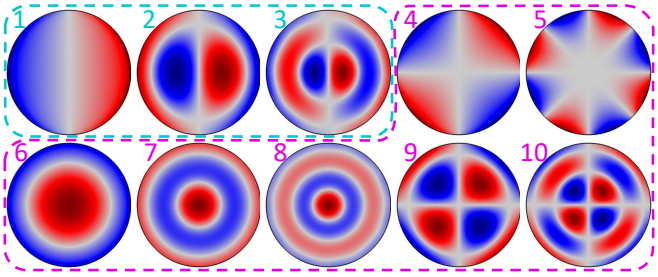

FIG. 4. Surface current density on the silver nanodisk relative to some radiative and non-radiative peaks, which are numbered respectively in cyan and magenta in Figure 3. These plots were obtained by the excitation of the modes on the structure with a specific orientation of the emitter, either a dipole or a quadrupole. For example, the mode 1 can be obtained with a dipole oriented along the X axis but also with the quadrupole $\hat{\mathbf{Q}}_{xz}$, while the mode 10 can only be obtained with quadrupoles, with for example $\hat{\mathbf{Q}}_{xx}$ and $\hat{\mathbf{Q}}_{xy}$.

First of all, our results obtained for the ED two-quanta transition where the emitter is placed on-axis (top left and top right spectra) correspond to the results in [48] with their analytical calculation of Purcell factors with a plasmon wave function formalism, thus confirming our method. Furthermore, the 2ED and 2EQ transitions are strongly enhanced by the plasmonic disk. Indeed, with the 25 nm diameter disk (left spectra) at $\omega = \omega_{eg}/2$, i.e., the frequency where both photons have the same energy, the 2ED and 2EQ transition rates are enhanced by, respectively, 8 and 15 orders of magnitude for the emission of two plasmons (dotted red line) and by, respectively, a factor $1.12 \times 10^5 (\pm 0.4\%)$ and $7.5 \times 10^{11} (\pm 5\%)$ for the emission of two photons (solid blue line). The standard deviation, expressed in percent, has been calculated by computing the COMSOL models at this frequency with finer mesh parameters.

Concerning the comparison of the different spectra, the surface current density of some modes excited on the disk is plotted in Figure 4. We first observe that the 2EQ spectrum relative to a 25 nm diameter disk (bottom left spectrum) has an additional non-radiative peak compared to the 2ED one (top left spectrum) that corresponds to a quadrupolar mode (cf. mode number 4 in Figure 4). Second, when the emitter is shifted (central spectra), the breaking of the azimuthal symmetry of the system leads to a greater wealth of excited modes (cf. non-radiative modes number 4 and 5 in Figure 4, note that the mode 5 peak is weakly visible at the scale of the figure), but the central radiative peak is slightly reduced. Note that in the off-axis configuration (central spectra), the 2ED spectra (top central spectrum) exhibits a peak (mode 4) corresponding to a quadrupolar mode excited on the structure, which was not possible to excite in the more symmetric on-axis configuration (top left spectrum). Third, when the diameter of the disk increases (right spectra), the frequency of the peaks changes and new, both radiative and non-radiative, peaks appear, which correspond to higher order modes (cf. modes number 2, 3, 7, 8, 9 and 10 in Figure 4). Remark for example that the dipolar mode 1 appears multiple times, such as in Fig. 3 top left and top right. The modes at these peaks have the same shape (Fig. 4), but there is a frequency shift because of the different disk radius. Note that only the bright peaks would show up in scattering spectra [61–63].

V. CONCLUSION

We develop a general framework to efficiently calculate two-photon spontaneous emission spectra of a quantum emitter in the vicinity of an arbitrary shaped nanostructure. It is based on the analytical calculation of the emitter contribution and, for the environment, on the classical computation of Purcell factors related to one-photon spontaneous emission. The latter are calculated by modelling classical point emitters in electromagnetic simulations, thus facilitating more complex geometries without available analytical models. Moreover, our framework goes beyond the dipolar approximation by taking into account the second-order multipolar interactions and is therefore relevant for plasmonic nano- and picocavities in which light is highly confined. In addition, our framework allows to calculate separately the radiative and non-radiative emission channels, which is important to distinguish for many applications.

As a direct application we use the COMSOL Multiphysics® software to show an enhancement of 5 and 11 orders of magnitude for the electric dipole and quadrupole two-photon transitions for the $s \to s$ transition of a hydrogen-like emitter placed under a plasmonic silver nanodisk. Subsequently, the flexibility of our framework allows the optimization and the design of platforms for efficient entangled two-photon sources, as an alternative to the conventional parametric down-conversion sources. These devices can include periodic structures in order to enhance the photon pair emission rate in the far-field [64]. For on-chip sources one proposes nanostructures joined to waveguides [65], photonic crystals [66], or cavities [67] in order to create an integrated two-photon source. The method can be used to study two-photon spontaneous process for diverse quantum emitters and can be extended for example by including interference between the multipolar emission channels of this process [28].

ACKNOWLEDGMENTS

We acknowledge support from the FRS-FNRS (Research project T.0166.20) and from Action de Recherche Concertée (project ARC-21/25 UMONS2).

[1] P. Dirac, The quantum theory of the emission and absorption of radiation, Proc. R. Soc. Lond. A **114**, 243 (1927).

[2] C. Cohen-Tannoudji, J. Dupont-Roc, and G. Grynberg, *Atom—Photon Interactions: Basic Process and Appilcations*, 1st ed. (Wiley, 1998).

[3] P. W. Milonni, Why spontaneous emission?, American Journal of Physics **52**, 340 (1984).

[4] W. Demtröder, *Atoms, Molecules and Photons*, Graduate Texts in Physics (Springer Berlin Heidelberg, Berlin, Heidelberg, 2010).

[5] E. M. Purcell, H. C. Torrey, and R. V. Pound, Resonance Absorption by Nuclear Magnetic Moments in a Solid, Physical Review **69**, 37 (1946).

[6] L. Novotny and B. Hecht, *Principles of Nano-Optics*, 2nd ed. (Cambridge University Press, Cambridge, 2012).

[7] M. Thomas, J.-J. Greffet, R. Carminati, and J. R. Arias-Gonzalez, Single-molecule spontaneous emission close to absorbing nanostructures, Applied Physics Letters **85**, 3863 (2004).

[8] M. Born and E. Wolf, *Principles of optics: electromagnetic theory of propagation, interference and diffraction of light*, 7th ed. (Cambridge University Press, Cambridge ; New York, 1999).

[9] C. Cohen-Tannoudji, B. Diu, and F. Laloë, *Quantum mechanics. Volume 1: Basic concepts, tools, and applications*, second edition ed. (Wiley-VCH Verlag GmbH & Co. KGaA, Weinheim, 2020).

[10] N. Rivera, I. Kaminer, B. Zhen, J. D. Joannopoulos, and M. Soljačić, Shrinking light to allow forbidden transitions on the atomic scale, Science **353**, 263 (2016).

[11] M. L. Andersen, S. Stobbe, A. S. Sørensen, and P. Lodahl, Strongly modified plasmon–matter interaction with mesoscopic quantum emitters, Nature Physics **7**, 215 (2011).

[12] P. Tighineanu, M. Andersen, A. Sørensen, S. Stobbe, and P. Lodahl, Probing Electric and Magnetic Vacuum Fluctuations with Quantum Dots, Physical Review Letters **113**, 043601 (2014).

[13] P. Tighineanu, A. Sørensen, S. Stobbe, and P. Lodahl, Unraveling the Mesoscopic Character of Quantum Dots in Nanophotonics, Physical Review Letters **114**, 247401 (2015).

[14] Y. Zhang, Z.-C. Dong, and J. Aizpurua, Influence of the Chemical Structure on Molecular Light Emission in Strongly Localized Plasmonic Fields, The Journal of Physical Chemistry C **124**, 4674 (2020).

[15] N. Rivera and I. Kaminer, Light–matter interactions with photonic quasiparticles, Nature Reviews Physics **2**, 538 (2020).

[16] M. Soljačić and J. D. Joannopoulos, Enhancement of nonlinear effects using photonic crystals, Nature Materials **3**, 211 (2004).

[17] D. Dovzhenko, V. Krivenkov, I. Kriukova, P. Samokhvalov, A. Karaulov, and I. Nabiev, Enhanced spontaneous emission from two-photon-pumped quantum dots in a porous silicon microcavity, Optics Letters **45**, 5364 (2020).

[18] P. K. Jain, D. Ghosh, R. Baer, E. Rabani, and A. P. Alivisatos, Near-field manipulation of spectroscopic selection rules on the nanoscale, Proceedings of the National Academy of Sciences **109**, 8016 (2012).

[19] A. M. Kern and O. J. F. Martin, Strong enhancement of forbidden atomic transitions using plasmonic nanostructures, Physical Review A **85**, 022501 (2012).

[20] V. Yannopapas and E. Paspalakis, Giant enhancement of dipole-forbidden transitions via lattices of plasmonic nanoparticles, Journal of Modern Optics **62**, 1435 (2015).

[21] F. Marquier, C. Sauvan, and J.-J. Greffet, Revisiting Quantum Optics with Surface Plasmons and Plasmonic Resonators, ACS Photonics **4**, 2091 (2017).

[22] S. Sanders, A. May, A. Alabastri, and A. Manjavacas, Extraordinary Enhancement of Quadrupolar Transitions Using Nanostructured Graphene, ACS Photonics **5**, 3282 (2018).

[23] J. Sloan, N. Rivera, J. D. Joannopoulos, I. Kaminer, and M. Soljačić, Controlling spins with surface magnon polaritons, Physical Review B **100**, 235453 (2019).

[24] D. S. Wang, T. Neuman, and P. Narang, Spin Emitters beyond the Point Dipole Approximation in Nanomagnonic Cavities, The Journal of Physical Chemistry C **125**, 6222 (2021).

[25] N. Rivera, G. Rosolen, J. D. Joannopoulos, I. Kaminer, and M. Soljačić, Making two-photon processes dominate one-photon processes using mid-IR phonon polaritons, Proceedings of the National Academy of Sciences **114**, 13607 (2017).

[26] N. Rivera, T. Christensen, and P. Narang, Phonon Polaritonics in Two-Dimensional Materials, Nano Letters **19**, 2653 (2019).

[27] T. Neuman, R. Esteban, D. Casanova, F. J. García-Vidal, and J. Aizpurua, Coupling of Molecular Emitters and Plasmonic Cavities beyond the Point-Dipole Approximation, Nano Letters **18**, 2358 (2018).

[28] E. Rusak, J. Straubel, P. Gładysz, M. Göddel, A. Kędziorski, M. Kühn, F. Weigend, C. Rockstuhl, and K. Słowik, Enhancement of and interference among higher order multipole transitions in molecules near a plasmonic nanoantenna, Nature Communications **10**, 5775 (2019).

[29] M. Kosik, O. Burlayenko, C. Rockstuhl, I. Fernandez-Corbaton, and K. Słowik, Interaction of atomic systems with quantum vacuum beyond electric dipole approximation, Scientific Reports **10**, 5879 (2020).

[30] G. Rosolen and B. Maes, Strong multipolar transition enhancement with graphene nanoislands, APL Photonics **6**, 086103 (2021).

[31] M. Göppert-Mayer, Über Elementarakte mit zwei Quantensprüngen, Annalen der Physik **401**, 273 (1931).

[32] G. Breit and E. Teller, Metastability of Hydrogen and Helium Levels., The Astrophysical Journal **91**, 215 (1940).

[33] L. J. Spitzer and J. L. Greenstein, Continuous Emission from Planetary Nebulae, The Astrophysical Journal **114**, 407 (1951).

[34] H. Krüger and A. Oed, Measurement of the decay-probability of metastable hydrogen by two-photon emission, Physics Letters A **54**, 251 (1975).

[35] S. P. Goldman and G. W. F. Drake, Relativistic two-photon decay rates of $2\,s_{1/2}$ hydrogenic ions, Physical Review A **24**, 183 (1981).

[36] Y. Ota, S. Iwamoto, N. Kumagai, and Y. Arakawa, Spontaneous Two-Photon Emission from a Single Quantum

Dot, Physical Review Letters **107**, 233602 (2011).
[37] A. Hayat, P. Ginzburg, and M. Orenstein, High-rate entanglement source via two-photon emission from semiconductor quantum wells, Physical Review B **76**, 035339 (2007).
[38] A. Hayat, P. Ginzburg, and M. Orenstein, Observation of two-photon emission from semiconductors, Nature Photonics **2**, 238 (2008).
[39] H. M. van Driel, On the path to entanglement, Nature Photonics **2**, 212 (2008).
[40] A. Nevet, N. Berkovitch, A. Hayat, P. Ginzburg, S. Ginzach, O. Sorias, and M. Orenstein, Plasmonic Nanoantennas for Broad-Band Enhancement of Two-Photon Emission from Semiconductors, Nano Letters **10**, 1848 (2010).
[41] F. Hu, L. Li, Y. Liu, Y. Meng, M. Gong, and Y. Yang, Two-plasmon spontaneous emission from a nonlocal epsilon-near-zero material, Communications Physics **4**, 84 (2021).
[42] A. N. Poddubny, P. Ginzburg, P. A. Belov, A. V. Zayats, and Y. S. Kivshar, Tailoring and enhancing spontaneous two-photon emission using resonant plasmonic nanostructures, Physical Review A **86**, 033826 (2012).
[43] A. Hayat, A. Nevet, P. Ginzburg, and M. Orenstein, Applications of two-photon processes in semiconductor photonic devices: invited review, Semiconductor Science and Technology **26**, 083001 (2011).
[44] A. Hayat, P. Ginzburg, and M. Orenstein, Entangled Photon Spectroscopy and Communications Based on Semiconductor Two-Photon Process, in *International Conference on Quantum Information* (OSA, Rochester, New York, 2007) p. JWC63.
[45] J. Zhang, J. Ma, M. Parry, M. Cai, R. Camacho-Morales, L. Xu, D. N. Neshev, and A. A. Sukhorukov, Spatially entangled photon pairs from lithium niobate nonlocal metasurfaces, Science Advances **8**, eabq4240 (2022).
[46] J. E. Ehrlich, X. L. Wu, I.-Y. S. Lee, Z.-Y. Hu, H. Röckel, S. R. Marder, and J. W. Perry, Two-photon absorption and broadband optical limiting with bis-donor stilbenes, Optics Letters **22**, 1843 (1997).
[47] Y. Muniz, F. S. S. da Rosa, C. Farina, D. Szilard, and W. J. M. Kort-Kamp, Quantum two-photon emission in a photonic cavity, Physical Review A **100**, 023818 (2019).
[48] Y. Muniz, A. Manjavacas, C. Farina, D. Dalvit, and W. Kort-Kamp, Two-Photon Spontaneous Emission in Atomically Thin Plasmonic Nanostructures, Physical Review Letters **125**, 033601 (2020).
[49] S. Smeets, B. Maes, and G. Rosolen, A general framework for two-photon spontaneous emission near plasmonic structures: supplementary notes (2023).
[50] D. P. Craig and T. Thirunamachandran, *Molecular quantum electrodynamics: an introduction to radiation-molecule interactions* (Academic Press, London ; Orlando, 1984).
[51] L. D. Barron and C. G. Gray, The multipole interaction Hamiltonian for time dependent fields, Journal of Physics A: Mathematical, Nuclear and General **6**, 59 (1973).
[52] P. W. Milonni, *The quantum vacuum: an introduction to quantum electrodynamics* (Academic Press, Boston, 1994).
[53] C. Cohen-Tannoudji, B. Diu, and F. Laloë, *Quantum mechanics. Volume 3: Fermions, bosons, photons, correlations and entanglement*, first edition ed. (Wiley-VCH GmbH & Co. KGaA, Weinheim, 2020).
[54] J. D. Jackson, *Classical electrodynamics*, 3rd ed. (Wiley, New York, 1999).
[55] A. Zangwill, *Modern electrodynamics* (Cambridge University Press, Cambridge, 2013).
[56] S. Y. Buhmann, *Dispersion Forces I*, Springer Tracts in Modern Physics, Vol. 247 (Springer Berlin Heidelberg, Berlin, Heidelberg, 2012).
[57] J.-M. Jin, *The finite element method in electromagnetics*, third edition ed. (John Wiley & Sons Inc, Hoboken. New Jersey, 2014).
[58] A. Taflove and S. C. Hagness, *Computational electrodynamics: the finite-difference time-domain method*, 3rd ed., Artech House antennas and propagation library (Artech House, Boston, 2005).
[59] M. C. Bottorff, G. J. Ferland, and J. P. Straley, Two-Photon Transitions and Continuous Emission from Hydrogenic Species, Publications of the Astronomical Society of the Pacific **118**, 1176 (2006).
[60] R. D. Cowan, *The theory of atomic structure and spectra*, Los Alamos series in basic and applied sciences No. 3 (University of California Press, Berkeley, 1981).
[61] S. Thongrattanasiri, F. H. L. Koppens, and F. J. García De Abajo, Complete Optical Absorption in Periodically Patterned Graphene, Physical Review Letters **108**, 047401 (2012).
[62] Z. Fang, S. Thongrattanasiri, A. Schlather, Z. Liu, L. Ma, Y. Wang, P. M. Ajayan, P. Nordlander, N. J. Halas, and F. J. García De Abajo, Gated Tunability and Hybridization of Localized Plasmons in Nanostructured Graphene, ACS Nano **7**, 2388 (2013).
[63] A. D. Kondorskiy, N. T. Lam, and V. S. Lebedev, Absorption and Scattering of Light by Silver and Gold Nanodisks and Nanoprisms, Journal of Russian Laser Research **39**, 56 (2018).
[64] J. Feng, Y.-F. Liu, Y.-G. Bi, and H.-B. Sun, Light manipulation in organic light-emitting devices by integrating micro/nano patterns: Light manipulation in organic light-emitting devices by integrating micro/nano patterns, Laser & Photonics Reviews **11**, 1600145 (2017).
[65] G. P. Agrawal, *Nonlinear fiber optics*, 4th ed., Quantum electronics–principles and applications (Elsevier / Academic Press, Amsterdam ; Boston, 2007).
[66] Y. Zeng, Y. Fu, X. Chen, W. Lu, and H. Ågren, Highly efficient generation of entangled photon pair by spontaneous parametric downconversion in defective photonic crystals, Journal of the Optical Society of America B **24**, 1365 (2007).
[67] A. Dousse, J. Suffczyński, A. Beveratos, O. Krebs, A. Lemaître, I. Sagnes, J. Bloch, P. Voisin, and P. Senellart, Ultrabright source of entangled photon pairs, Nature **466**, 217 (2010).

Supplementary Notes
A general framework for two-photon spontaneous emission near plasmonic nanostructures

S. Smeets,* B. Maes,† and G. Rosolen‡
Micro- and Nanophotonic Materials Group, Research Institute for Materials Science and Engineering, University of Mons, 20 Place du Parc, Mons B-7000, Belgium
(Dated: March 27, 2023)

* Steve.Smeets@umons.ac.be
† Bjorn.Maes@umons.ac.be
‡ Gilles.Rosolen@umons.ac.be

I. TWO-PHOTON SPONTANEOUS EMISSION RATE

In this section we present the derivation of the 2EQ (two-electric quadrupole) emission channel contribution to the two-photon spontaneous emission (TPSE) rate. Subsequently, we calculate it in free-space. For the 2ED (two-electric dipole) and the 2MD (two-magnetic dipole) contributions the derivations are similar and are therefore not presented here. The reader is invited to see the derivation of the 2ED transition rate in [1, 2]. In order to calculate transitions rates we use Fermi's golden rule as a perturbative approach.

A. Fermi's golden rule

As mentioned in the main text, the probability per unit time that a system carries out a second-order transition by emitting two quanta from an initial state $|i\rangle$ to a final state $|f\rangle$, upon an interaction described by the Hamiltonian $H_{\rm int}$, is given by Fermi's golden rule [1, 3]:

$$\Gamma^{(2)}_{i\to f} = \frac{2\pi}{\hbar}|M^{(2)}_{fi}|^2\delta(E_f - E_i) \tag{I.1}$$

with the second-order matrix element

$$M^{(2)}_{fi} = \sum_l \frac{\langle f|\, H_{\rm int}\, |l\rangle\, \langle l|\, H_{\rm int}\, |i\rangle}{E_i - E_l} \tag{I.2}$$

where the summation runs over all possible virtual intermediate states $|l\rangle$ of the system. In these equations $\hbar$ is the reduced Planck constant, E_a stands for the energy of the system in the state $|a\rangle$ with $a = i, l, f$, and the superscript (2) indicates that this is a second-order transition, in contrast with first-order transitions. Furthermore, this second-order transition can be seen as two successive transitions in which each one emits a quantum (Figure I.1).

Regarding the states in this second-order process [1], the initial one is characterized by the emitter in an excited state $|e\rangle$ and the field in the vacuum state $|\text{vac}\rangle$, while in the final one the emitter is in a lower energy state $|g\rangle$ and the field is in a two-quanta state $|1_\alpha, 1_{\alpha'}\rangle$. Thus, they are respectively written as

$$|i\rangle = |e; \text{vac}\rangle \tag{I.3a}$$
$$\text{and as } |f\rangle = |g; 1_\alpha, 1_{\alpha'}\rangle\,. \tag{I.3b}$$

In the intermediate states that connect these two states, the emitter is in an intermediate energy state $|m\rangle$ and the field is in a one-quantum state. Further on, the energy of the emitter in the state $|a\rangle$ will be denoted as ε_a with $a = e, m, g$. Depending on in which mode is the emitted quantum, the intermediate states are written as

$$|l\rangle = |m; 1_\alpha\rangle \tag{I.4a}$$
$$\text{or as } |l\rangle = |m; 1_{\alpha'}\rangle\,. \tag{I.4b}$$

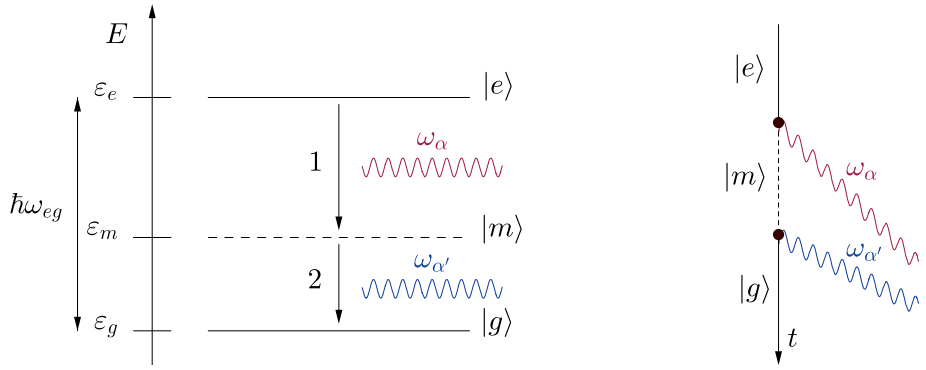

FIG. I.1. Energy and time representations of a second-order transition. The emitter carries-out a first transition from its excited state $|e\rangle$ to a virtual intermediate state $|m\rangle$ by emitting a photon in the mode α. Then, a second transition is carried out to the ground state $|g\rangle$ of lower energy by emitting a photon in the mode α'. The transition energy is given by $\hbar\omega_{eg} := \varepsilon_e - \varepsilon_g$. These representations only consider the intermediate state of the system $|l\rangle = |m; 1_\alpha\rangle$ where the first photon is emitted in the mode α, but similar representations can be sketched by inverting the role of the two emitted quanta.

B. Derivation of the 2EQ transition rate

Now that we have introduced Fermi's golden rule and all states involved in this second-order transition, let us derive the 2EQ transition rate. Given that the initial and the final energies of the system are, respectively, $E_i = \varepsilon_e$ and $E_f = \varepsilon_g + \hbar\omega_\alpha + \hbar\omega_{\alpha'}$, the Dirac delta distribution in Fermi's golden rule in equation (I.1) can be rewritten as

$$\delta(E_f - E_i) = \frac{1}{\hbar}\delta(\omega_{eg} - \omega_\alpha - \omega_{\alpha'}) \tag{I.5}$$

where we define $\omega_{ab} := (\varepsilon_a - \varepsilon_b)/\hbar$ with $a, b = e, m, g$.

Then, given that there are two kinds of intermediate states (cf. equations (I.4)), the summation over them in the expression of the second-order matrix element $M_{fi}^{(2)}$ is split in two:

$$\begin{aligned} M_{fi}^{(2)} = &\sum_m \frac{\langle 1_\alpha, 1_{\alpha'}| \langle \varepsilon_g| H_{\text{int}} |\varepsilon_m\rangle |1_\alpha\rangle \langle 1_\alpha| \langle \varepsilon_m| H_{\text{int}} |\varepsilon_e\rangle |\text{vac}\rangle}{\hbar(\omega_{em} - \omega_\alpha)} \\ &+ \sum_m \frac{\langle 1_\alpha, 1_{\alpha'}| \langle \varepsilon_g| H_{\text{int}} |\varepsilon_m\rangle |1_{\alpha'}\rangle \langle 1_{\alpha'}| \langle \varepsilon_m| H_{\text{int}} |\varepsilon_e\rangle |\text{vac}\rangle}{\hbar(\omega_{em} - \omega_{\alpha'})} \end{aligned} \tag{I.6}$$

where the first summation corresponds to the representations sketched in Figure I.1.

At this point we have not yet assumed a specific transition. Let us now consider a 2EQ transition, i.e., a transition during which two successive electric quadrupole transitions occur. As a reminder the electric quadrupole interaction Hamiltonian [4, 5] is given by

$$H_{\text{EQ}}(\mathbf{R}, t) = -\mathbf{Q} : [\nabla \mathbf{E}(\mathbf{R}, t)] \tag{I.7}$$

with $\mathbf{Q}$ the electric quadrupole moment operator, $\nabla = (\frac{\partial}{\partial x}, \frac{\partial}{\partial y}, \frac{\partial}{\partial z})^T$ a column vector where T denotes the transpose, $\mathbf{E}$ the electric field operator, and $\mathbf{R}$ the emitter position taken at the center of its charge distribution. In this equation the dot product is the vector scalar product, the product $\nabla\mathbf{E}$ is an outer product, whereas the double dot product is defined as $\mathbf{T} : \mathbf{U} := \sum_{ij} T_{\ldots ij} U_{ji\ldots}$ with $\mathbf{T}$ and $\mathbf{U}$ two tensors of rank greater or equal to two.

The electric field operator can be written as a function of the normal modes $\mathbf{A}_\alpha(\mathbf{r})$ of the vector potential [6, 7]:

$$\mathbf{E}(\mathbf{r}, t) = i\sum_\alpha \sqrt{\frac{\hbar\omega_\alpha}{2\varepsilon_0}} \left\{ a_\alpha(t)\mathbf{A}_\alpha(\mathbf{r}) - a_\alpha^\dagger(t)\mathbf{A}_\alpha^*(\mathbf{r}) \right\} \tag{I.8}$$

where ε_0 is the vacuum electric permittivity and where $a_\alpha(t)$ and $a_\alpha^\dagger(t)$ are the annihilation and the creation operators of a photon in the mode α of energy $\hbar\omega_\alpha$. Note that the modes $\mathbf{A}_\alpha(\mathbf{r})$ are normalized and form a complete set of solutions of the Helmholtz equation subjected to the boundary conditions imposed by the photonic environment. These are also the conditions applied to the modes that lead to the Purcell effect.

Let us now calculate the factor $\langle 1_\alpha, 1_{\alpha'}| \langle \varepsilon_g| H_{\text{int}} |\varepsilon_m\rangle |1_\alpha\rangle$ that appears in equation (I.6) with the interaction Hamiltonian given in equation (I.7) and with the electric field operator given in equation (I.8). As we are interested in emission processes only the part of $\mathbf{E}$ involving creation operators, noted as $\mathbf{E}^{(-)}$, is kept in this calculation:

$$\langle 1_\alpha, 1_{\alpha'}| \langle \varepsilon_g| H_{\text{EQ}} |\varepsilon_m\rangle |1_\alpha\rangle = -\langle \varepsilon_g| \mathbf{Q} |\varepsilon_m\rangle : \left[\nabla \langle 1_\alpha, 1_{\alpha'}| \mathbf{E}^{(-)}(\mathbf{R}) |1_\alpha\rangle\right] \tag{I.9a}$$

$$= -\mathbf{Q}^{gm} : \left[\nabla \langle 1_\alpha, 1_{\alpha'}| - i\sum_\beta \sqrt{\frac{\hbar\omega_\beta}{2\varepsilon_0}} a_\beta^\dagger \mathbf{A}_\beta^*(\mathbf{R}) |1_\alpha\rangle\right] \tag{I.9b}$$

where $\mathbf{Q}^{ab} := \langle a|\mathbf{Q}|b\rangle$ stands for the transition electric quadrupole moment (i.e., the first-order matrix element of $\mathbf{Q}$) that describes the emitter's transition from the state $|b\rangle$ to the state $|a\rangle$ (a, $b = e$, m, g). In the previous equation only the term involving the creation operator that creates a photon in the mode $\beta = \alpha'$ leads to a non-zero term because the field states form an orthonormal basis[1]. Thus, we get

$$\langle 1_\alpha, 1_{\alpha'}| \langle \varepsilon_g| H_{\text{EQ}} |\varepsilon_m\rangle |1_\alpha\rangle = i\sqrt{\frac{\hbar\omega_{\alpha'}}{2\varepsilon_0}} \mathbf{Q}^{gm} : [\nabla \mathbf{A}_{\alpha'}^*(\mathbf{R})] \underbrace{\langle 1_\alpha, 1_{\alpha'}| a_{\alpha'}^\dagger |1_\alpha\rangle}_{\langle 1_\alpha, 1_{\alpha'}|1_\alpha, 1_{\alpha'}\rangle = 1} \tag{I.10a}$$

$$= i\sqrt{\frac{\hbar\omega_{\alpha'}}{2\varepsilon_0}} \mathbf{Q}^{gm} : [\nabla \mathbf{A}_{\alpha'}^*(\mathbf{R})]\,. \tag{I.10b}$$

[1] An orthonormal basis satisfies $\langle 1_\alpha|1_\beta\rangle = \delta_{\alpha\beta}$ and $\langle 1_\alpha, 1_{\alpha'}|1_\beta, 1_{\beta'}\rangle = \langle 1_\alpha|1_\beta\rangle \langle 1_{\alpha'}|1_{\beta'}\rangle = \delta_{\alpha\beta}\,\delta_{\alpha'\beta'}$.

Similar developments for the second factor in the first summation of equation (I.6) lead to

$$\langle 1_\alpha| \langle \varepsilon_m| H_{\mathrm{EQ}} |\varepsilon_e\rangle |\mathrm{vac}\rangle = i\sqrt{\frac{\hbar\omega_\alpha}{2\varepsilon_0}}\mathbf{Q}^{me} : [\nabla \mathbf{A}^*_\alpha(\mathbf{R})]. \tag{I.11}$$

Therefore, the first summation in equation (I.6) is rewritten as

$$-\frac{\sqrt{\omega_\alpha\omega_{\alpha'}}}{2\varepsilon_0}\sum_m \frac{\mathbf{Q}^{gm} : [\nabla \mathbf{A}^*_{\alpha'}(\mathbf{R})]\ \mathbf{Q}^{me} : [\nabla \mathbf{A}^*_\alpha(\mathbf{R})]}{\omega_{em}-\omega_\alpha}. \tag{I.12}$$

Concerning the second summation presents in equation (I.6), the result can be obtained by inverting the role of α and α' in the last obtained equation. Thus, the second-order matrix element $M^{(2)}_{fi}$ is rewritten as

$$M^{(2)}_{fi} = -\frac{\sqrt{\omega_\alpha\omega_{\alpha'}}}{2\varepsilon_0}\sum_m \left\{ \frac{\mathbf{Q}^{gm} : [\nabla \mathbf{A}^*_{\alpha'}(\mathbf{R})]\ \mathbf{Q}^{me} : [\nabla \mathbf{A}^*_\alpha(\mathbf{R})]}{\omega_{em}-\omega_\alpha} + \frac{\mathbf{Q}^{gm} : [\nabla \mathbf{A}^*_\alpha(\mathbf{R})]\ \mathbf{Q}^{me} : [\nabla \mathbf{A}^*_{\alpha'}(\mathbf{R})]}{\omega_{em}-\omega_{\alpha'}} \right\} \tag{I.13}$$

and since the double dot product of two second rank tensors is commutative, one obtains

$$M^{(2)}_{fi} = -\frac{\sqrt{\omega_\alpha\omega_{\alpha'}}}{2\varepsilon_0}\sum_m \left\{ \frac{[\nabla \mathbf{A}^*_{\alpha'}(\mathbf{R})] : \mathbf{Q}^{gm}\mathbf{Q}^{me} : [\nabla \mathbf{A}^*_\alpha(\mathbf{R})]}{\omega_{em}-\omega_\alpha} + \frac{[\nabla \mathbf{A}^*_\alpha(\mathbf{R})] : \mathbf{Q}^{gm}\mathbf{Q}^{me} : [\nabla \mathbf{A}^*_{\alpha'}(\mathbf{R})]}{\omega_{em}-\omega_{\alpha'}} \right\} \tag{I.14a}$$

$$= -\frac{\sqrt{\omega_\alpha\omega_{\alpha'}}}{2\varepsilon_0}[\nabla \mathbf{A}^*_{\alpha'}(\mathbf{R})] : \sum_m \left\{ \frac{\mathbf{Q}^{gm}\mathbf{Q}^{me}}{\omega_{em}-\omega_\alpha} + \frac{\mathbf{Q}^{gm}\mathbf{Q}^{me}}{\omega_{em}-\omega_{\alpha'}} \right\} : [\nabla \mathbf{A}^*_\alpha(\mathbf{R})]. \tag{I.14b}$$

Therefore, the complex conjugate of $M^{(2)}_{fi}$ is given by[2]

$$\left(M^{(2)}_{fi}\right)^* = -\frac{\sqrt{\omega_\alpha\omega_{\alpha'}}}{2\varepsilon_0}[\nabla \mathbf{A}_{\alpha'}(\mathbf{R})] : \sum_m \left\{ \frac{\mathbf{Q}^{mg}\mathbf{Q}^{em}}{\omega_{em}-\omega_\alpha} + \frac{\mathbf{Q}^{mg}\mathbf{Q}^{em}}{\omega_{em}-\omega_{\alpha'}} \right\} : [\nabla \mathbf{A}_\alpha(\mathbf{R})] \tag{I.15}$$

that we can rearrange as follows

$$\left(M^{(2)}_{fi}\right)^* = -\frac{\sqrt{\omega_\alpha\omega_{\alpha'}}}{2\varepsilon_0}[\nabla \mathbf{A}_\alpha(\mathbf{R})] : \underbrace{\sum_m \left\{ \frac{\mathbf{Q}^{em}\mathbf{Q}^{mg}}{\omega_{em}-\omega_\alpha} + \frac{\mathbf{Q}^{em}\mathbf{Q}^{mg}}{\omega_{em}-\omega_{\alpha'}} \right\}}_{\boldsymbol{\mathcal{Q}}^{eg}(\omega_\alpha,\omega_{\alpha'})} : [\nabla \mathbf{A}_{\alpha'}(\mathbf{R})]. \tag{I.16}$$

In the last equation we define the fourth rank tensor $\boldsymbol{\mathcal{Q}}^{eg}$ as

$$\boldsymbol{\mathcal{Q}}^{eg}(\omega_\alpha,\omega_{\alpha'}) := \sum_m \left(\frac{\mathbf{Q}^{em}\,\mathbf{Q}^{mg}}{\omega_{em}-\omega_\alpha} + \frac{\mathbf{Q}^{mg}\,\mathbf{Q}^{em}}{\omega_{em}-\omega_{\alpha'}} \right) \tag{I.17}$$

where the outer product is implied. The components of the tensor that come from the outer product of two tensors $\mathbf{U}$ and $\mathbf{V}$ are $(\mathbf{UV})_{i_1,i_2,\ldots,i_n,j_1,j_2,\ldots,j_n} := U_{i_1,i_2,\ldots,i_n}V_{j_1,j_2,\ldots,j_n}$. It describes the two successive electric quadrupole transitions of the emitter between the states $|e\rangle$ and $|g\rangle$ of the emitter. Subsequently, we will refer to it as the second-order transition electric quadrupole moment. Note that since $\mathbf{Q}$ is symmetric, the fourth rank tensor $\boldsymbol{\mathcal{Q}}^{eg}$ is also symmetric:

$$\begin{cases} \mathcal{Q}^{eg}_{ijkl} = \mathcal{Q}^{eg}_{jikl} & \forall i,j,k,l = 1,2,3 \quad \text{(I.18a)} \\ \mathcal{Q}^{eg}_{ijkl} = \mathcal{Q}^{eg}_{ijlk} & \forall i,j,k,l = 1,2,3. \quad \text{(I.18b)} \end{cases}$$

Moreover, since $\mathbf{Q}$ can be taken traceless [8, 9], given the definition of $\boldsymbol{\mathcal{Q}}^{eg}$, it satisfies the two following properties:

$$\begin{cases} \sum_{i=1}^{3} \mathcal{Q}^{eg}_{iikl} = 0 & \forall k,l = 1,2,3 \quad \text{(I.19a)} \\ \sum_{k=1}^{3} \mathcal{Q}^{eg}_{ijkk} = 0 & \forall i,j = 1,2,3. \quad \text{(I.19b)} \end{cases}$$

---

[2] For an Hermitian operator: $(\mathbf{Q}^{ab})^* = (\langle a|\mathbf{Q}|b\rangle)^* = \langle b|\mathbf{Q}^\dagger|a\rangle = \langle b|\mathbf{Q}|a\rangle = \mathbf{Q}^{ba}$ where the dagger denotes the operation of taking the transpose and the complex conjugate.

Let us now take the square modulus of $M_{fi}^{(2)}$:

$$\left|M_{fi}^{(2)}\right|^2 = \left|\left(M_{fi}^{(2)}\right)^*\right|^2 = \frac{\omega_\alpha \omega_{\alpha'}}{4\varepsilon_0^2} \left|[\nabla \mathbf{A}_\alpha(\mathbf{R})] : \boldsymbol{\mathcal{Q}}^{eg}(\omega_\alpha, \omega_{\alpha'}) : [\nabla \mathbf{A}_{\alpha'}(\mathbf{R})]\right|^2 \tag{I.20}$$

that can be directly injected, together with equation (I.5), in Fermi's golden rule given in equation (I.1):

$$\Gamma_{\mathrm{2EQ}}^{(2)}(\mathbf{R}) = \frac{2\pi}{\hbar^2} \frac{\omega_\alpha \omega_{\alpha'}}{4\varepsilon_0^2} \left|[\nabla \mathbf{A}_\alpha(\mathbf{R})] : \boldsymbol{\mathcal{Q}}^{eg}(\omega_\alpha, \omega_{\alpha'}) : [\nabla \mathbf{A}_{\alpha'}(\mathbf{R})]\right|^2 \delta(\omega_{eg} - \omega_\alpha - \omega_{\alpha'}). \tag{I.21}$$

As a final step we take the summation over all possible states for the two emitted quanta. However, due to the quantum permutation symmetry, we must take into account a factor 1/2 to avoid double counting. We finally get the 2EQ contribution to the total two-photon spontaneous emission rate:

$$\boxed{\Gamma_{\mathrm{2EQ}}^{(2)}(\mathbf{R}) = \frac{\pi}{4\varepsilon_0^2\hbar^2} \sum_{\alpha,\alpha'} \omega_\alpha \omega_{\alpha'} \left|[\nabla \mathbf{A}_\alpha(\mathbf{R})] : \boldsymbol{\mathcal{Q}}^{eg}(\omega_\alpha, \omega_{\alpha'}) : [\nabla \mathbf{A}_{\alpha'}(\mathbf{R})]\right|^2 \delta(\omega_{eg} - \omega_\alpha - \omega_{\alpha'}).} \tag{I.22}$$

The derived equation is valid regardless of the emitter environment. Now, as a direct application we derive the 2EQ transition rate in vacuum.

C. 2EQ transition rate in free-space

In vacuum the field modes are plane waves defined by a wave vector $\mathbf{k}$ and a unitary polarization vector $\boldsymbol{\varepsilon}_{\mathbf{k},s}$ where the parameter $s = 1, 2$ represents the two transverse polarizations [1, 6]. Consequently, the field modes in equation (I.22) become

$$\mathbf{A}_\alpha(\mathbf{r}) \longrightarrow \mathbf{A}_{\mathbf{k},s}(\mathbf{r}) = \frac{e^{i\mathbf{k}\cdot\mathbf{r}}}{\sqrt{V}} \boldsymbol{\varepsilon}_{\mathbf{k},s} \tag{I.23}$$

where V stands for the arbitrary and finite box quantization volume in which the field is assumed to be confined. In addition, the angular frequency ω_α becomes ω_k and the summation over the modes α becomes $\sum_{s=1}^{2} \sum_{\mathbf{k}}$. By taking the continuum limit the summation over the wave vectors $\mathbf{k}$ is replaced by an integral [1, 6]:

$$\sum_{s=1}^{2} \sum_{\mathbf{k}} \overset{V\to\infty}{\longrightarrow} \frac{V}{(2\pi)^3} \sum_{s=1}^{2} \int \mathrm{d}^3 k = \frac{V}{(2\pi)^3} \sum_{s=1}^{2} \int k^2 \, \mathrm{d}k \, \mathrm{d}\Omega_k \tag{I.24}$$

where we switched to spherical coordinates in the reciprocal space with $\mathrm{d}\Omega_k = \sin\theta_k \, \mathrm{d}\theta_k \, \mathrm{d}\phi_k$ the element of solid angle in $\mathbf{k}$-space.

Let us now calculate the transition rate given in equation (I.22) by carrying out the replacement given in equation (I.24) as well as by calculating the following outer product:

$$\nabla \mathbf{A}_{\mathbf{k},s}(\mathbf{r}) = i\mathbf{k} \frac{e^{i\mathbf{k}\cdot\mathbf{r}}}{\sqrt{V}} \boldsymbol{\varepsilon}_{\mathbf{k},s}. \tag{I.25}$$

Thereby, the transition rate is given by

$$\Gamma_{\mathrm{2EQ},0}^{(2)}(\mathbf{R}) = \frac{\pi}{4\varepsilon_0^2\hbar^2} \frac{V^2}{(2\pi)^6} \sum_{s,s'=1}^{2} \int\int \omega_k \omega_{k'} \left| \left[i\mathbf{k} \frac{e^{i\mathbf{k}\cdot\mathbf{R}}}{\sqrt{V}} \boldsymbol{\varepsilon}_{\mathbf{k},s} \right] : \boldsymbol{\mathcal{Q}}^{eg}(\omega_k, \omega_{k'}) : \left[i\mathbf{k}' \frac{e^{i\mathbf{k}'\cdot\mathbf{R}}}{\sqrt{V}} \boldsymbol{\varepsilon}_{\mathbf{k}',s'} \right] \right|^2$$
$$\times \delta(\omega_{eg} - \omega_k - \omega_{k'}) \, k^2 k'^2 \, \mathrm{d}k \, \mathrm{d}k' \, \mathrm{d}\Omega_k \, \mathrm{d}\Omega_{k'} \tag{I.26a}$$

$$\Leftrightarrow \Gamma_{\mathrm{2EQ},0}^{(2)} = \frac{\pi}{4\varepsilon_0^2\hbar^2} \frac{1}{(2\pi)^6} \sum_{s,s'=1}^{2} \int\int \omega_k \omega_{k'} \, k^2 k'^2 \left| [\mathbf{k} \, \boldsymbol{\varepsilon}_{\mathbf{k},s}] : \boldsymbol{\mathcal{Q}}^{eg}(\omega_k, \omega_{k'}) : [\mathbf{k}' \, \boldsymbol{\varepsilon}_{\mathbf{k}',s'}] \right|^2$$
$$\times \delta(\omega_{eg} - \omega_k - \omega_{k'}) \, \mathrm{d}k \, \mathrm{d}k' \, \mathrm{d}\Omega_k \, \mathrm{d}\Omega_{k'} \tag{I.26b}$$

where the transition rate is now independent of the emitter position $\mathbf{R}$ due to the homogeneity of space and where the subscript 0 reminds that the emission is in free-space. By using the free-space dispersion relation $\omega_k = ck$, we can make the following replacements:

$$\begin{cases} \mathbf{k} = k\,\hat{\mathbf{k}} & \text{(I.27a)} \\ k = \dfrac{\omega_k}{c} & \text{(I.27b)} \\ \mathrm{d}k = \dfrac{1}{c}\mathrm{d}\omega_k & \text{(I.27c)} \end{cases}$$

where the caret denotes unitary vectors. These replacements lead to

$$\Gamma^{(2)}_{2\mathrm{EQ},0} = \frac{\pi}{4\varepsilon_0^2\hbar^2}\frac{1}{(2\pi)^6 c^{10}}\sum_{s,s'=1}^{2}\int\int \omega_k^5\omega_{k'}^5 \left|\left[\hat{\mathbf{k}}\,\boldsymbol{\varepsilon}_{\mathbf{k},s}\right] : \boldsymbol{\mathcal{Q}}^{eg}(\omega_k,\omega_{k'}) : \left[\hat{\mathbf{k}'}\,\boldsymbol{\varepsilon}_{\mathbf{k}',s'}\right]\right|^2 \delta(\omega_{eg}-\omega_k-\omega_{k'})\,\mathrm{d}\omega_k\,\mathrm{d}\omega_{k'}\,\mathrm{d}\Omega_k\,\mathrm{d}\Omega_{k'}. \tag{I.28}$$

Let us now develop the double dot products as well as the square modulus:

$$\begin{aligned}\Gamma^{(2)}_{2\mathrm{EQ},0} = \frac{\pi}{4\varepsilon_0^2\hbar^2}\frac{1}{(2\pi)^6 c^{10}}\sum_{s,s'=1}^{2}\int\int &\omega_k^5\omega_{k'}^5\,\hat{\mathrm{k}}_j\,\hat{\mathrm{k}}'_l\,\hat{\mathrm{k}}_b\,\hat{\mathrm{k}}'_d\,\varepsilon_{\mathbf{k},s,i}\,\varepsilon_{\mathbf{k}',s',k}\,\varepsilon^*_{\mathbf{k},s,a}\,\varepsilon^*_{\mathbf{k}',s',c}\,\mathcal{Q}^{eg}_{ijkl}(\mathcal{Q}^{eg}_{abcd})^* \\ &\times\delta(\omega_{eg}-\omega_k-\omega_{k'})\,\mathrm{d}\omega_k\,\mathrm{d}\omega_{k'}\,\mathrm{d}\Omega_k\,\mathrm{d}\Omega_{k'}\end{aligned} \tag{I.29}$$

where the Einstein summation convention is used, the frequency dependencies have been omitted, and $\hat{\mathbf{k}}$ and $\hat{\mathbf{k}'}$ are real vectors (in general, polarization vectors can be complex vectors). As the set $\left\{\boldsymbol{\varepsilon}_{\mathbf{k},1},\boldsymbol{\varepsilon}_{\mathbf{k},2},\hat{\mathbf{k}}\right\}$ forms an orthonormal basis, we can use the closure relation

$$\sum_{s=1}^{2}\boldsymbol{\varepsilon}_{\mathbf{k},s}\,\boldsymbol{\varepsilon}^*_{\mathbf{k},s} + \hat{\mathbf{k}}\,\hat{\mathbf{k}} = \mathbb{1}_{3\times3} \tag{I.30a}$$

$$\Leftrightarrow \sum_{s=1}^{2}\varepsilon_{\mathbf{k},s,i}\,\varepsilon^*_{\mathbf{k},s,j} = \delta_{ij} - \hat{\mathrm{k}}_i\,\hat{\mathrm{k}}_j \tag{I.30b}$$

where $\mathbb{1}_{3\times3}$ is identity matrix in three dimensions and where $\varepsilon_{\mathbf{k},s,i}$ and $\hat{\mathrm{k}}_i$ denote, respectively, the components in spherical coordinates of the unitary vectors $\boldsymbol{\varepsilon}_{\mathbf{k},s}$ and $\hat{\mathbf{k}}$ ($i = 1,2,3$). By using the last equation we can calculate the following integrals:

$$\begin{aligned}&\int\int \hat{\mathrm{k}}_j\,\hat{\mathrm{k}}_b\,\hat{\mathrm{k}}'_l\,\hat{\mathrm{k}}'_d\sum_s\varepsilon_{\mathbf{k},s,i}\,\varepsilon^*_{\mathbf{k},s,a}\sum_{s'}\varepsilon_{\mathbf{k}',s',k}\,\varepsilon^*_{\mathbf{k}',s',c}\,d\Omega_k\,\mathrm{d}\Omega_{k'} \\ &\quad= \int\int \hat{\mathrm{k}}_j\,\hat{\mathrm{k}}_b\,\hat{\mathrm{k}}'_l\,\hat{\mathrm{k}}'_d\,(\delta_{ia}-\hat{\mathrm{k}}_i\,\hat{\mathrm{k}}_a)\,(\delta_{kc}-\hat{\mathrm{k}}_k\,\hat{\mathrm{k}}_c)\,d\Omega_k\,\mathrm{d}\Omega_{k'} &\text{(I.31a)} \\ &\quad= \delta_{ia}\,\delta_{kc}\int\hat{\mathrm{k}}_j\hat{\mathrm{k}}_b\,\mathrm{d}\Omega_k\int\hat{\mathrm{k}}'_l\hat{\mathrm{k}}'_d\,\mathrm{d}\Omega_{k'} - \delta_{ia}\int\hat{\mathrm{k}}_j\hat{\mathrm{k}}_b\,\mathrm{d}\Omega_k\int\hat{\mathrm{k}}'_k\hat{\mathrm{k}}'_l\hat{\mathrm{k}}'_c\hat{\mathrm{k}}'_d\,\mathrm{d}\Omega_{k'} \\ &\quad- \delta_{kc}\int\hat{\mathrm{k}}_i\hat{\mathrm{k}}_j\hat{\mathrm{k}}_a\hat{\mathrm{k}}_b\,\mathrm{d}\Omega_k\int\hat{\mathrm{k}}'_l\hat{\mathrm{k}}'_d\,\mathrm{d}\Omega_{k'} + \int\hat{\mathrm{k}}_i\hat{\mathrm{k}}_j\hat{\mathrm{k}}_a\hat{\mathrm{k}}_b\,\mathrm{d}\Omega_k\int\hat{\mathrm{k}}'_k\hat{\mathrm{k}}'_l\hat{\mathrm{k}}'_c\hat{\mathrm{k}}'_d\,\mathrm{d}\Omega_{k'}. &\text{(I.31b)}\end{aligned}$$

One can show that [8]:

$$\int_{4\pi}\hat{\mathrm{k}}_i\hat{\mathrm{k}}_j\,\mathrm{d}\Omega_k = \frac{4\pi}{3}\delta_{ij}, \tag{I.32a}$$

$$\int_{4\pi}\hat{\mathrm{k}}_i\hat{\mathrm{k}}_j\hat{\mathrm{k}}_k\hat{\mathrm{k}}_l\,\mathrm{d}\Omega_k = \frac{4\pi}{15}\left(\delta_{ij}\delta_{kl}+\delta_{ik}\delta_{jl}+\delta_{il}\delta jk\right). \tag{I.32b}$$

Let us now multiply the obtained result by the product $\mathcal{Q}_{ijkl}\mathcal{Q}^*_{abcd}$, which depends only on the angular frequencies and not on the solid angles. After a few lines one shows that

$$\int\int \hat{\mathrm{k}}_j\,\hat{\mathrm{k}}_b\,\hat{\mathrm{k}}'_l\,\hat{\mathrm{k}}'_d\sum_s\varepsilon_{\mathbf{k},s,i}\,\varepsilon^*_{\mathbf{k},s,a}\sum_{s'}\varepsilon_{\mathbf{k}',s',k}\,\varepsilon^*_{\mathbf{k}',s',c}\,d\Omega_k\,\mathrm{d}\Omega_{k'}\,\mathcal{Q}^{eg}_{ijkl}(\mathcal{Q}^{eg}_{abcd})^* = \left(\frac{4\pi}{5}\right)^2\|\boldsymbol{\mathcal{Q}}^{eg}\|^2. \tag{I.33}$$

To obtain the last result we use equations (I.18) and (I.19) and define the norm of a rank-n tensor $\mathbf{U}$ with $n \geq 1$ as $\|\mathbf{U}\|^2 := \sum_{i_1,i_2,\ldots,i_n} |U_{i_1,i_2,\ldots,i_n}|^2$.

Let us use the obtained result into the equation of the transition rate:

$$\Gamma^{(2)}_{2\mathrm{EQ},0} = \frac{1}{400\pi^3\varepsilon_0^2\hbar^2c^{10}} \int\int \omega_k^5\omega_{k'}^5 \ \|\boldsymbol{\mathcal{Q}}^{eg}(\omega_k,\omega_{k'})\|^2 \ \delta(\omega_{eg}-\omega_k-\omega_{k'})\,\mathrm{d}\omega_k\,\mathrm{d}\omega_{k'}. \tag{I.34}$$

The integration can be solved with the following change of variables:

$$\begin{cases} W = \omega_k + \omega_{k'} & \text{(I.35a)} \\ \omega = \omega_k & \text{(I.35b)} \\ \mathrm{d}\omega_k\,\mathrm{d}\omega_{k'} = \mathrm{d}W\,\mathrm{d}\omega. & \text{(I.35c)} \end{cases}$$

Thus, the transition rate can be rewritten as

$$\Gamma^{(2)}_{2\mathrm{EQ},0} = \frac{1}{400\pi^3\varepsilon_0^2\hbar^2c^{10}} \int\int \omega^5(W-\omega)^5 \ \|\boldsymbol{\mathcal{Q}}^{eg}(\omega,W-\omega)\|^2 \ \delta(\omega_{eg}-W)\,\mathrm{d}\omega\,\mathrm{d}W \tag{I.36a}$$

$$= \frac{1}{400\pi^3\varepsilon_0^2\hbar^2c^{10}} \int \omega^5(\omega_{eg}-\omega)^5 \ \|\boldsymbol{\mathcal{Q}}^{eg}(\omega,\omega_{eg}-\omega)\|^2 \ \mathrm{d}\omega. \tag{I.36b}$$

Thereby, since the energy of an emitted photon is within the range 0 and $\hbar\omega_{eg}$, the 2EQ contribution to the two-photon spontaneous emission in free-space is given by

$$\Gamma^{(2)}_{2\mathrm{EQ},0} = \int_0^{\omega_{eg}} \gamma^{(2)}_{\mathrm{EQ},0}(\omega)\,\mathrm{d}\omega \tag{I.37}$$

with $\gamma^{(2)}_{\mathrm{EQ},0}(\omega)$ the free-space spectral distribution of the emitted photons:

$$\boxed{\gamma^{(2)}_{2\mathrm{EQ},0}(\omega) = \frac{1}{400\pi^3\varepsilon_0^2\hbar^2c^{10}}\omega^5(\omega_{eg}-\omega)^5 \ \|\boldsymbol{\mathcal{Q}}^{eg}(\omega_k,\omega_{eg}-\omega_k)\|^2\,.} \tag{I.38}$$

As the spontaneous emission takes place in vacuum, the calculated rate is independent of the emitter position.

---

[1] D. P. Craig and T. Thirunamachandran, *Molecular quantum electrodynamics: an introduction to radiation-molecule interactions* (Academic Press, London ; Orlando, 1984).

[2] Y. Muniz, F. S. S. da Rosa, C. Farina, D. Szilard, and W. J. M. Kort-Kamp, Quantum two-photon emission in a photonic cavity, Physical Review A **100**, 023818 (2019).

[3] C. Cohen-Tannoudji, J. Dupont-Roc, and G. Grynberg, *Atom—Photon Interactions: Basic Process and Appilcations*, 1st ed. (Wiley, 1998).

[4] L. D. Barron and C. G. Gray, The multipole interaction Hamiltonian for time dependent fields, Journal of Physics A: Mathematical, Nuclear and General **6**, 59 (1973).

[5] L. Novotny and B. Hecht, *Principles of Nano-Optics*, 2nd ed. (Cambridge University Press, Cambridge, 2012).

[6] P. W. Milonni, *The quantum vacuum: an introduction to quantum electrodynamics* (Academic Press, Boston, 1994).

[7] C. Cohen-Tannoudji, B. Diu, and F. Laloë, *Quantum mechanics. Volume 3: Fermions, bosons, photons, correlations and entanglement*, first edition ed. (Wiley-VCH GmbH & Co. KGaA, Weinheim, 2020).

[8] J. D. Jackson, *Classical electrodynamics*, 3rd ed. (Wiley, New York, 1999).

[9] A. Zangwill, *Modern electrodynamics* (Cambridge University Press, Cambridge, 2013).

II. RELATION BETWEEN THE TPSE RATES AND PURCELL FACTORS

In the main text we outline the main steps leading to the expression of the two-electric dipole (2ED), the two-magnetic dipole (2MD) and the two-electric quadrupole (2EQ) transition rates as a function of the one-photon Purcell factors. Here the complete derivation is presented for the 2EQ transition. To this end the idea is first of all to express the 2EQ transition rate as a function of the dyadic Green's function $\mathbf{G}$, and to normalize it by the free-space one. Concerning the Green's function, its imaginary part admits a spectral representation that can be expanded in terms of the normal modes $\mathbf{A}_\alpha$ of the electromagnetic field [1]:

$$\mathrm{Im}\mathbf{G}(\omega;\mathbf{r},\mathbf{r}') = \frac{\pi c^2}{2\omega}\sum_\alpha \mathbf{A}_\alpha(\mathbf{r})\mathbf{A}^*_\alpha(\mathbf{r}')\,\delta(\omega-\omega_\alpha). \tag{II.1}$$

Then, to simplify the obtained equation, some properties and a modified version of the Voigt notation are used. Finally, the connection between the Green's function and the Purcell factors is made by looking at the one-photon spontaneous emission rate with different electric quadrupole transition moment orientations. Let us start with a reminder about the 2EQ transition rate, for which the full derivation is presented in the first section of this document.

A. Reminder

The general expression of the 2EQ transition rate, as well as the one related to vacuum, is given by

$$\Gamma^{(2)}_{\mathrm{2EQ}}(\mathbf{R}) = \frac{\pi}{4\varepsilon_0^2\hbar^2}\sum_{\alpha,\alpha'}\omega_\alpha\omega_{\alpha'}\left|[\nabla\mathbf{A}_\alpha(\mathbf{R})]:\boldsymbol{\mathcal{Q}}^{eg}(\omega_\alpha,\omega_{\alpha'}):[\nabla\mathbf{A}_{\alpha'}(\mathbf{R})]\right|^2\delta(\omega_{eg}-\omega_\alpha-\omega_{\alpha'}), \tag{II.2a}$$

$$\Gamma^{(2)}_{\mathrm{2EQ},0} = \int_0^{\omega_{eg}}\gamma^{(2)}_{\mathrm{2EQ},0}(\omega)\,\mathrm{d}\omega, \qquad \gamma^{(2)}_{\mathrm{2EQ},0}(\omega) = \frac{\omega^5(\omega_{eg}-\omega)^5}{400\pi^3\varepsilon_0^2\hbar^2c^{10}}\left\|\boldsymbol{\mathcal{Q}}^{eg}(\omega,\omega_{eg}-\omega)\right\|^2. \tag{II.2b}$$

In these equations $\hbar$ is the reduced Plank constant, ε_0 represents the vacuum electric permittivity, c denotes the speed of light in vacuum, $\mathbf{R}$ stands for the emitter's position taken at the center of its charge distribution, ω_α is the angular frequency of the photon in the normal mode $\mathbf{A}_\alpha$ of the electromagnetic field, $\hbar\omega_{eg} := \varepsilon_e - \varepsilon_g$ represents the transition energy, and $\boldsymbol{\mathcal{Q}}^{eg}$ stands for second-order transition electric quadrupole moment that describes the emitter's transition between its excited state $|e\rangle$ and its ground state $|g\rangle$. Moreover, $\nabla = (\frac{\partial}{\partial x},\frac{\partial}{\partial y},\frac{\partial}{\partial z})^T$ is a column vector with T denoting the transpose, the product $\nabla\mathbf{A}_\alpha$ is an outer product, whereas the double dot product is defined as $\mathbf{T}:\mathbf{U} := \sum_{i,j}T_{\ldots ij}U_{ji\ldots}$ with $\mathbf{T}$ and $\mathbf{U}$ two tensors of rank greater than or equal to two. In addition, the squared norm of a rank-n tensor $\mathbf{U}$ with $n\in\mathbb{N}_0$ has been defined as $\|\mathbf{U}\|^2 := \sum_{i_1,i_2,\ldots,i_n}|U_{i_1,i_2,\ldots,i_n}|^2$.

B. Expression as a function of the dyadic Green's function

Let us start the developments in order to connect with the Green's function, given in equation (II.1), for the photon emitted at frequency $\omega_{\alpha'} = \omega_{eg}-\omega_\alpha$ [2]:

$$\Gamma^{(2)}_{\mathrm{2EQ}}(\mathbf{R}) = \frac{\pi}{4\varepsilon_0^2\hbar^2}\sum_{\alpha,\alpha'}\omega_\alpha\omega_{\alpha'}\left(\partial_j A_{\alpha,i}\mathcal{Q}_{ijab}(\omega_\alpha,\omega_{\alpha'})\partial_b A_{\alpha',a}\right)\left(\partial_l A_{\alpha,k}\mathcal{Q}_{klcd}(\omega_\alpha,\omega_{\alpha'})\partial_d A_{\alpha',c}\right)^*\delta(\omega_{eg}-\omega_\alpha-\omega_{\alpha'}) \tag{II.3a}$$

$$= \frac{\pi}{4\varepsilon_0^2\hbar^2}\sum_\alpha\omega_\alpha(\omega_{eg}-\omega_\alpha)\mathcal{Q}_{ijab}(\omega_\alpha,\omega_{eg}-\omega_\alpha)\mathcal{Q}^*_{klcd}(\omega_\alpha,\omega_{eg}-\omega_\alpha)\partial_j A_{\alpha,i}\partial_l A^*_{\alpha,k} \times\sum_{\alpha'}\partial_b A_{\alpha',a}\partial_d A^*_{\alpha',c}\delta(\omega_{eg}-\omega_\alpha-\omega_{\alpha'}) \tag{II.3b}$$

$$= \frac{\pi}{4\varepsilon_0^2\hbar^2}\sum_\alpha\omega_\alpha(\omega_{eg}-\omega_\alpha)\mathcal{Q}_{ijab}(\omega_\alpha,\omega_{eg}-\omega_\alpha)\mathcal{Q}^*_{klcd}(\omega_\alpha,\omega_{eg}-\omega_\alpha)\partial_j A_{\alpha,i}\partial_l A^*_{\alpha,k} \times\left\{\partial_b\partial_{d'}\sum_{\alpha'}A_{\alpha',a}(\mathbf{r})\partial_d A^*_{\alpha',c}(\mathbf{r}')\delta(\omega_{eg}-\omega_\alpha-\omega_{\alpha'})\right\}_{\mathbf{r}=\mathbf{r}'=\mathbf{R}} \tag{II.3c}$$

$$= \frac{1}{2\varepsilon_0^2\hbar^2c^2}\sum_\alpha\omega_\alpha(\omega_{eg}-\omega_\alpha)^2\mathcal{Q}_{ijab}(\omega_\alpha,\omega_{eg}-\omega_\alpha)\mathcal{Q}^*_{klcd}(\omega_\alpha,\omega_{eg}-\omega_\alpha)\partial_j A_{\alpha,i}\partial_l A^*_{\alpha,k} \times\left\{\partial_b\partial_{d'}\mathrm{Im}G_{ac}(\omega_{eg}-\omega_\alpha;\mathbf{r},\mathbf{r}')\right\}_{\mathbf{r}=\mathbf{r}'=\mathbf{R}} \tag{II.3d}$$

where ∂_i and $\partial_{i'}$ mean derivatives with respect to the coordinates $\mathbf{r}$ and $\mathbf{r}'$, respectively, where the Einstein summation convention is used, and where the eg subscript and the spatial dependency have been omitted.

By using the property $f(\omega_\alpha) = \int_{-\infty}^{\infty} f(\omega)\,\delta(\omega-\omega_\alpha)\,\mathrm{d}\omega$, we obtain

$$\Gamma^{(2)}_{\mathrm{2EQ}}(\mathbf{R}) = \frac{1}{2\varepsilon_0^2\hbar^2c^2}\int_{-\infty}^{\infty}\omega(\omega_{eg}-\omega)^2\mathcal{Q}_{ijab}(\omega,\omega_{eg}-\omega)\mathcal{Q}^*_{klcd}(\omega,\omega_{eg}-\omega) \times\sum_\alpha \partial_j A_{\alpha,i}\partial_l A^*_{\alpha,k}\delta(\omega-\omega_\alpha)\left\{\partial_b\partial_{d'}\mathrm{Im}G_{ac}(\omega_{eg}-\omega;\mathbf{r},\mathbf{r}')\right\}_{\mathbf{r}=\mathbf{r}'=\mathbf{R}}\mathrm{d}\omega \tag{II.4a}$$

$$= \frac{1}{\pi\varepsilon_0^2\hbar^2c^4}\int_0^{\omega_{eg}}\omega^2(\omega_{eg}-\omega)^2\mathcal{Q}_{ijab}(\omega,\omega_{eg}-\omega)\mathcal{Q}^*_{klcd}(\omega,\omega_{eg}-\omega) \times\left\{\partial_j\partial_{l'}\mathrm{Im}G_{ik}(\omega;\mathbf{r},\mathbf{r}')\right\}_{\mathbf{r}=\mathbf{r}'=\mathbf{R}}\left\{\partial_b\partial_{d'}\mathrm{Im}G_{ac}(\omega_{eg}-\omega;\mathbf{r},\mathbf{r}')\right\}_{\mathbf{r}=\mathbf{r}'=\mathbf{R}}\mathrm{d}\omega \tag{II.4b}$$

where the Green's function appears (related to the photon emitted at the frequency ω), and where the integration limits have been adapted since the frequency of a photon is within the range comprised between 0 and ω_{eg}.

Let us now divide the spectral distribution $\gamma^{(2)}_{\mathrm{2EQ}}(\omega;\mathbf{R})$, i.e., the integrand of the last equation, by the one related to free-space given in equation (II.2b):

$$\frac{\gamma^{(2)}_{\mathrm{2EQ}}(\omega;\mathbf{R})}{\gamma^{(2)}_{\mathrm{2EQ},0}(\omega)} = \hat{\mathcal{Q}}^{eg}_{ijab}(\omega,\omega_{eg}-\omega)\left(\hat{\mathcal{Q}}^{eg}_{klcd}(\omega,\omega_{eg}-\omega)\right)^* T_{ijkl}(\omega;\mathbf{R})\,T_{abcd}(\omega_{eg}-\omega;\mathbf{R}). \tag{II.5}$$

In the last equation we have defined the normalized second-order transition electric quadrupole moment $\hat{\boldsymbol{\mathcal{Q}}}^{eg}$ and the fourth rank tensor $\mathbf{T}$ respectively as

$$\hat{\boldsymbol{\mathcal{Q}}}^{eg}(\omega,\omega_{eg}-\omega) := \frac{\boldsymbol{\mathcal{Q}}^{eg}(\omega,\omega_{eg}-\omega)}{\|\boldsymbol{\mathcal{Q}}^{eg}(\omega,\omega_{eg}-\omega)\|}, \tag{II.6a}$$

$$T_{ijkl}(\omega;\mathbf{R}) := \frac{20\pi c^3}{\omega^3}\left\{\partial_j\partial_{l'}\mathrm{Im}G_{ik}(\omega;\mathbf{r},\mathbf{r}')\right\}_{\mathbf{r}=\mathbf{r}'=\mathbf{R}}. \tag{II.6b}$$

Since $\mathbf{T}$ is a real tensor, by using equation (II.1), we can show that it satisfies the property $\forall i,j,k,l=1,2,3 : T_{ijkl} = T_{klij}$. Notice that the indices i,j,k and l are related to the photon emitted at the frequency ω while the indices a,b,c and d concern the photon emitted at the complementary frequency $\omega_{eg}-\omega$. Unfortunately, the derived equation contains 9^4 terms but a few properties can be used to reduce this number.

C. Simplification

Let us use the three following properties in order to reduce the number of terms in equation (II.5):

$$\boldsymbol{\mathcal{Q}}^{eg}_{ijab} = \boldsymbol{\mathcal{Q}}^{eg}_{jiab} = \boldsymbol{\mathcal{Q}}^{eg}_{ijba} = \boldsymbol{\mathcal{Q}}^{eg}_{jiba} \qquad \forall i,j,a,b=1,2,3, \tag{II.7a}$$

$$\sum_{i=1}^{3}\boldsymbol{\mathcal{Q}}^{eg}_{iiab} = \sum_{a=1}^{3}\boldsymbol{\mathcal{Q}}^{eg}_{ijaa} = 0 \qquad \forall i,j,a,b=1,2,3, \tag{II.7b}$$

$$T_{ijkl} = T_{klij} \qquad \forall i,j,k,l=1,2,3. \tag{II.7c}$$

The first one is the symmetry property of the fourth rank tensor $\boldsymbol{\mathcal{Q}}^{eg}$, the second one comes from the traceless property of one-order transition electric quadrupole moments, while the last one is derived from equation (II.6b).

Firstly, the first property is used to suppress the redundance over the symmetric components of the tensor $\boldsymbol{\mathcal{Q}}^{eg}$. This provides an expression involving 6^4 terms instead of 9^4:

$$\frac{\gamma^{(2)}_{\mathrm{2EQ}}(\omega;\mathbf{R})}{\gamma^{(2)}_{\mathrm{2EQ},0}(\omega)} = \sum_{\mu,\nu=1}^{6}\sum_{\alpha,\beta=1}^{6}\hat{\mathcal{Q}}^{eg}_{\mu\alpha}(\omega,\omega_{eg}-\omega)\left(\hat{\mathcal{Q}}^{eg}_{\nu\beta}(\omega,\omega_{eg}-\omega)\right)^* U_{\mu\nu}(\omega;\mathbf{R})\,U_{\alpha\beta}(\omega_{eg}-\omega;\mathbf{R}) \tag{II.8}$$

with

$$U_{\mu\nu} := \begin{cases} T_{\mu\nu} & \forall\mu,\nu=1,2,3 \\ T_{\mu\nu}+T_{\mu\bar{\nu}} & \forall\mu=1,2,3\ ;\ \nu=4,5,6 \\ T_{\mu\nu}+T_{\bar{\mu}\nu} & \forall\mu=4,5,6\ ;\ \nu=1,2,3 \\ T_{\mu\nu}+T_{\mu\bar{\nu}}+T_{\bar{\mu}\nu}+T_{\bar{\mu}\bar{\nu}} & \forall\mu,\nu=4,5,6. \end{cases} \tag{II.9}$$

To derive this equation we use the Voigt notation. This mathematical convention exploits the symmetry property of a tensor, by removing its redundant components, to represent it by a lower rank tensor defined in a higher dimensional space. In this way the second-order transition electric quadrupole moment, which is a fourth rank tensor in three dimensions, is represented as a second rank tensor in six dimensions:

$$(\mathcal{Q}_{ijab})_{3\times3\times3\times3} \rightarrow \begin{pmatrix} \mathcal{Q}_{1111} & \mathcal{Q}_{1122} & \mathcal{Q}_{1133} & \mathcal{Q}_{1123} & \mathcal{Q}_{1113} & \mathcal{Q}_{1112} \\ \mathcal{Q}_{2211} & \mathcal{Q}_{2222} & \mathcal{Q}_{2233} & \mathcal{Q}_{2223} & \mathcal{Q}_{2213} & \mathcal{Q}_{2212} \\ \mathcal{Q}_{3311} & \mathcal{Q}_{3322} & \mathcal{Q}_{3333} & \mathcal{Q}_{3323} & \mathcal{Q}_{3313} & \mathcal{Q}_{3312} \\ \mathcal{Q}_{2311} & \mathcal{Q}_{2322} & \mathcal{Q}_{2333} & \mathcal{Q}_{2323} & \mathcal{Q}_{2313} & \mathcal{Q}_{2312} \\ \mathcal{Q}_{1311} & \mathcal{Q}_{1322} & \mathcal{Q}_{1333} & \mathcal{Q}_{1323} & \mathcal{Q}_{1313} & \mathcal{Q}_{1312} \\ \mathcal{Q}_{1211} & \mathcal{Q}_{1222} & \mathcal{Q}_{1233} & \mathcal{Q}_{1223} & \mathcal{Q}_{1213} & \mathcal{Q}_{1212} \end{pmatrix} \rightarrow (\mathcal{Q}_{\mu\alpha})_{6\times6}\,. \tag{II.10}$$

The Table II.1 establishes the correspondence between the new indices and the ones of the represented tensor. Furthermore, in equation (II.9), the dependencies has been omitted and the bar over a pair of indices means taking the related symmetric one (e.g., $T_{2\overline{6}} = T_{22\overline{12}} = T_{2221}$).

(i,j)	$(1,1)$	$(2,2)$	$(3,3)$	$(2,3)$	$(1,3)$	$(1,2)$
μ	1	2	3	4	5	6

TABLE II.1. Voigt notation: correspondence between the pair of indices (i,j) of a symmetric tensor in three dimensions and the indices μ in six dimensions. The indices $\mu = 1,2,3$ correspond to the diagonal components of a second rank tensor, while the indices $\mu = 3,4,5$ correspond to its three independent off-diagonal components. By convention the indices of this notation are denoted with Greek letters.

Secondly, by using the second property linked to the traceless property, we obtain a formula involving 5^4 terms:

$$\frac{\gamma^{(2)}_{\text{2EQ}}(\omega;\mathbf{R})}{\gamma^{(2)}_{\text{2EQ},0}(\omega)} = \sum_{\substack{\mu,\nu=1\\ \mu,\nu\neq3}}^{6}\sum_{\substack{\alpha,\beta=1\\ \alpha,\beta\neq3}}^{6} \hat{\mathcal{Q}}^{eg}_{\mu\alpha}(\omega,\omega_{eg}-\omega)\left(\hat{\mathcal{Q}}^{eg}_{\nu\beta}(\omega,\omega_{eg}-\omega)\right)^{*} F^{\text{EQ}}_{\mu\nu}(\omega;\mathbf{R})\, F^{\text{EQ}}_{\alpha\beta}(\omega_{eg}-\omega;\mathbf{R}) \tag{II.11}$$

with

$$F^{\text{EQ}}_{\mu\nu} := \begin{cases} U_{\mu\nu} - U_{\mu3} - U_{3\nu} + U_{33} & \forall\mu,\nu = 1,2 \\ U_{\mu\nu} - U_{3\nu} & \forall\mu = 1,2 \quad ;\ \nu = 4,5,6 \\ U_{\mu\nu} - U_{\mu3} & \forall\mu = 4,5,6\ ;\ \nu = 1,2 \\ U_{\mu\nu} & \forall\mu,\nu = 4,5,6. \end{cases} \tag{II.12}$$

Thirdly, the last property implies that $V_{\mu\nu} = V_{\nu\mu}$, providing a final expression involving only $(\sum_{i=1}^{5} i)^2 = 15^2$ terms:

$$\boxed{\frac{\gamma^{(2)}_{\text{2EQ}}(\omega;\mathbf{R})}{\gamma^{(2)}_{\text{2EQ},0}(\omega)} = \sum_{\substack{\mu,\nu=1\\ \nu\geq\mu}}^{5}\sum_{\substack{\alpha,\beta=1\\ \beta\geq\alpha}}^{5} \hat{\mathcal{Q}}^{eg}_{\mu\alpha\nu\beta}(\omega,\omega_{eg}-\omega)\, F^{\text{EQ}}_{\mu\nu}(\omega;\mathbf{R})\, F^{\text{EQ}}_{\alpha\beta}(\omega_{eg}-\omega;\mathbf{R}).} \tag{II.13}$$

Note that the indices μ and ν are relative to the first quantum, while the indices α and β are relative to the second one. Also, the second rank tensor $\mathbf{F}^{\text{EQ}}$ in five dimensions is expressed as a function of the tensor $\mathbf{T}$, i.e., as a function of the imaginary part of the dyadic Green's function. In this equation the fourth rank tensor $\hat{\mathcal{Q}}^{eg}_{\mu\alpha\nu\beta}$ in five dimensions is defined as

$$\hat{\mathcal{Q}}_{\mu\alpha\nu\beta} := \begin{cases} \hat{\mathcal{Q}}_{\mu\alpha}\hat{\mathcal{Q}}^{*}_{\nu\beta} & \forall\mu = \nu\ ;\ \alpha = \beta \\ \hat{\mathcal{Q}}_{\mu\alpha}\hat{\mathcal{Q}}^{*}_{\nu\beta} + \hat{\mathcal{Q}}_{\mu\beta}\hat{\mathcal{Q}}^{*}_{\nu\alpha} & \forall\mu = \nu\ ;\ \alpha < \beta \\ \hat{\mathcal{Q}}_{\mu\alpha}\hat{\mathcal{Q}}^{*}_{\nu\beta} + \hat{\mathcal{Q}}_{\nu\alpha}\hat{\mathcal{Q}}^{*}_{\mu\beta} & \forall\mu < \nu\ ;\ \alpha = \beta \\ 2\,\hat{\mathcal{Q}}_{\mu\alpha}\hat{\mathcal{Q}}^{*}_{\nu\beta} + 2\,\hat{\mathcal{Q}}_{\mu\beta}\hat{\mathcal{Q}}^{*}_{\nu\alpha} & \forall\mu < \nu\ ;\ \alpha < \beta \end{cases} \tag{II.14}$$

where we use the relation $\hat{\mathcal{Q}}_{\mu\alpha}\hat{\mathcal{Q}}^{*}_{\nu\beta} = \hat{\mathcal{Q}}_{\nu\beta}\hat{\mathcal{Q}}^{*}_{\mu\alpha}$ (since this product must be real), and where we modified the Voigt notation to skip the last diagonal element of the second-order tensor. Thus, the third row and column have been removed in equation (II.10) as well as the third column in Table II.1 ($\mu = 3,4,5$ now corresponds to $(i,j) = (2,3),(1,3),(1,2)$).

D. Connection with Purcell factors

We first consider the one-photon EQ transition rate in order to establish the relation between the tensor $\mathbf{F}^{\mathrm{EQ}}$ and the one-photon Purcell factors, which are defined here as the ratio between the one-photon EQ transition rate and the corresponding rate in free-space. Similar developments lead to the EQ transition rate:

$$\frac{\Gamma^{(1)}_{\mathrm{EQ}}(\mathbf{R})}{\Gamma^{(1)}_{\mathrm{EQ},0}} = \sum_{\substack{\mu,\nu=1\\ \nu\geq\mu}}^{5} \hat{Q}^{eg}_{\mu\nu}\, F^{\mathrm{EQ}}_{\mu\nu}(\omega_{eg};\mathbf{R}) \tag{II.15}$$

with the second rank tensor $\hat{\mathbf{Q}}^{eg}$ in five dimensions defined as

$$\hat{Q}^{eg}_{\mu\nu} := \begin{cases} \hat{Q}^{eg}_{\mu}(\hat{Q}^{eg}_{\mu})^* & \forall \mu = \nu \\ 2\hat{Q}^{eg}_{\mu}(\hat{Q}^{eg}_{\nu})^* & \forall \mu < \nu \end{cases} \tag{II.16}$$

where we used the relation $\hat{Q}_\mu \hat{Q}^*_\nu = \hat{Q}_\nu \hat{Q}^*_\mu$, since this product must be real.

Let us now calculate using equation (II.15) the EQ transition rate for different quadrupole spatial configurations. Since a general electric quadrupole moment involves up to five independent components, it can be expanded on a basis of 5 quadrupoles. To construct this basis we consider two different types of quadrupoles, which are sketched in Figure II.1. In our notations these quadrupoles are represented by a vector in five dimensions where only the μ-th component is non-zero and equals to $1/\sqrt{2}$.

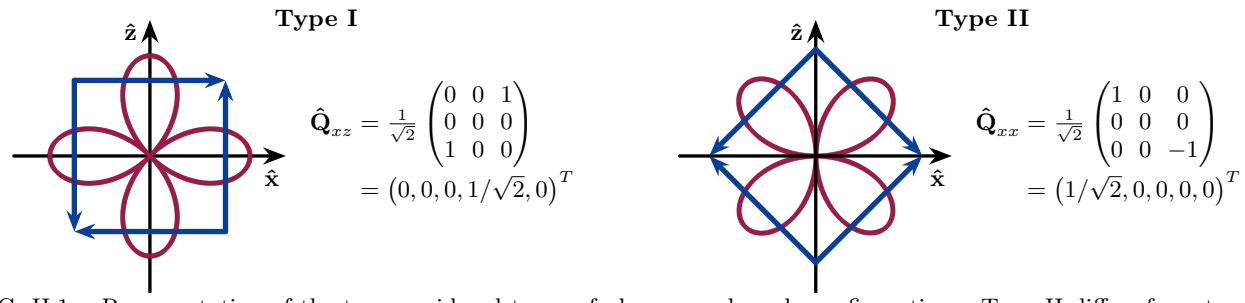

FIG. II.1. Representation of the two considered types of planar quadrupole configurations. Type II differs from type I by a rotation of 45° in the plane and involves only diagonal components, while type I involves solely off-diagonal components. They are represented by means of four dipoles of same norm (blue arrows) and the radiation patterns are sketched in dark red. The modified Voigt notation is used to represent their tensor by means of a five-dimensional vector.

First, we define five Purcell factors P^{EQ}_μ where the indices $\{\mu = 1,\ldots,5\}$ correspond, respectively, to the indices $\{xx, yy, yz, xz, xy\}$ (three types I and two types II[1]):

$$P^{\mathrm{EQ}}_\mu(\omega;\mathbf{R}) := \frac{1}{2} F^{\mathrm{EQ}}_{\mu\mu}(\omega;\mathbf{R}) \qquad \forall \mu = 1,\ldots,5. \tag{II.17}$$

These factors correspond to the ratio between the EQ transition rate of an emitter for which its transition electric quadrupole moment is the basis tensor $\hat{\mathbf{Q}}_\mu$ and the corresponding rate in free space.

Second, let us consider all of the possible combinations of the basis quadrupoles[2]:

$$\hat{\mathbf{Q}}_{\mu\nu} := \frac{1}{N}\left(\hat{\mathbf{Q}}_\mu + \hat{\mathbf{Q}}_\nu\right) \qquad \forall \mu,\nu = 1,\ldots,5\ ;\ \mu < \nu \tag{II.18}$$

with N a normalization constant. This allows us to define ten Purcell factors:

$$P^{\mathrm{EQ}}_{\mu\nu} := \begin{cases} \frac{1}{3}\left(P_\mu + P_\nu + F_{\mu\nu}\right) & \text{if } (\mu,\nu) = (1,2) \\ \frac{1}{2}\left(P_\mu + P_\nu + F_{\mu\nu}\right) & \forall \mu,\nu = 2,3,4,5\ ;\ \mu < \nu \end{cases} \tag{II.19}$$

---

[1] We do not need to consider the type II quadrupole $\hat{\mathbf{Q}}_{zz}$ because in our modified Voigt notation, we removed the last diagonal component to remove redundance with respect to the traceless property.

[2] Note that all considered quadrupoles need to be normalized and that the quadrupole $\hat{\mathbf{Q}}_{xxyy} = (\hat{\mathbf{Q}}_{xx} + \hat{\mathbf{Q}}_{yy})/\sqrt{3}$ is the linear quadrupole represented by the diagonal matrix $1/\sqrt{6}\,\mathrm{diag}(1,1,-2)$.

where the EQ superscript and the dependencies have been omitted, and where the Purcell factors $P^{\mathrm{EQ}}_{\mu\nu}$ are relative to an emitter that has its transition electric quadrupole moment described by the tensor $\hat{\mathbf{Q}}_{\mu\nu}$ (i.e., an equal and linear combination of the tensors $\hat{\mathbf{Q}}_{\mu}$ and $\hat{\mathbf{Q}}_{\nu}$).

To summarize, we established a relation between the 15 independent components of the symmetric tensor $\mathbf{F}^{\mathrm{EQ}}$, which are related to the derivatives of the imaginary part of the dyadic Green's function, and 15 Purcell factors:

$$F^{\mathrm{EQ}}_{\mu\nu}(\omega;\mathbf{R}) = \begin{cases} 2P^{\mathrm{EQ}}_{\mu} & \forall \mu = \nu \\ 3P^{\mathrm{EQ}}_{\mu\nu} - P^{\mathrm{EQ}}_{\mu} - P^{\mathrm{EQ}}_{\nu} & \text{if } (\mu,\nu) = (1,2) \\ 2P^{\mathrm{EQ}}_{\mu\nu} - P^{\mathrm{EQ}}_{\mu} - P^{\mathrm{EQ}}_{\nu} & \text{else} \end{cases} \tag{II.20}$$

where the dependencies have been omitted. Thus, in the most general case these 15 Purcell are necessary to calculate the 2EQ transition rate:

$$\left\{P^{\mathrm{EQ}}_{\mu}\right\} \cup \left\{P^{\mathrm{EQ}}_{\mu\nu}\right\} \tag{II.21}$$

where the indices $\mu,\nu = 1,\ldots,5$ with $\mu < \nu$ correspond to the indices $\{xx, yy, yz, xz, xy\}$. In vacuum all Purcell factors tend towards one and so $\mathbf{F}^{\mathrm{EQ}}$ is given by

$$F^{\mathrm{EQ}}_{\mu\nu} = \begin{cases} 2 & \forall \mu = \nu \\ 1 & \text{if } (\mu,\nu) = (1,2) \\ 0 & \text{else.} \end{cases} \tag{II.22}$$

---

[1] L. Novotny and B. Hecht, *Principles of Nano-Optics*, 2nd ed. (Cambridge University Press, Cambridge, 2012).

[2] A. Cuartero-González and A. I. Fernández-Domínguez, Light-Forbidden Transitions in Plasmon-Emitter Interactions beyond the Weak Coupling Regime, ACS Photonics **5**, 3415 (2018).

III. MULTIPOLAR SECOND-ORDER TRANSITION MOMENTS FOR A HYDROGEN ATOM

In the main text we derive the expressions of the two-photon spontaneous emission rates for the two-electric dipole (2ED), the two-magnetic dipole (2MD), and the two-electric quadrupole (2EQ) transitions. Each of these formulas involves a multipolar second-order transition moment that depends only on the electronic structure of the emitter. Here, the one related to the 2EQ transition is calculated analytically for a transition between two s states of the hydrogen atom. The reader is invited to consult the appendix of [1] for the derivation of the second-order electric dipole transition moment.

As a reminder, the second-order electric quadrupole transition moment between the excited state $|e\rangle$ and the ground state $|g\rangle$ of the emitter is defined as

$$\boldsymbol{\mathcal{Q}}^{eg}(\omega_\alpha,\omega_{\alpha'}) := \sum_m \left(\frac{\mathbf{Q}^{em}\,\mathbf{Q}^{mg}}{\omega_{em}-\omega_\alpha} + \frac{\mathbf{Q}^{mg}\,\mathbf{Q}^{em}}{\omega_{em}-\omega_{\alpha'}} \right) \tag{III.1}$$

and depends on the frequencies of both emitted quanta ω_α and $\omega_{\alpha'}$. In this equation $\hbar\omega_{em}$ is the transition energy between the excited state $|e\rangle$ and the intermediate state $|m\rangle$, while $\mathbf{Q}^{ab} := \langle a|\mathbf{Q}|b\rangle$ stands for the transition electric quadrupole moment that describes the emitter transition from the state $|b\rangle$ to the state $|a\rangle$ (a, $b = e$, m, g).

Since we assume that the emitter is a hydrogen atom, we know that its wavefunction $\psi(\mathbf{r})$ can be written as a product between a radial function $R_{N,L}(r)$ and a spherical harmonic function $Y_L^M(\theta,\varphi)$ [2]:

$$\psi(\mathbf{r}) = R_{N,L}(r)\,Y_L^M(\theta,\varphi) \tag{III.2}$$

where N, L and M are, respectively, the principal, azimuthal and magnetic quantum numbers. Moreover, we assume an $s \to s$ transition and, thereby, the excited and ground states are

$$|e\rangle = |N_e; L_e = 0; M_e = 0\rangle\,, \tag{III.3a}$$
$$|g\rangle = |N_g; L_g = 0; M_g = 0\rangle \tag{III.3b}$$

with $\{N_e, L_e, M_e\}$ and $\{N_g, L_g, M_g\}$ the quantum numbers which characterize, respectively, the excited and the ground states.

By using the appropriate selection rules, it is possible to deduce the nature of the intermediate states $|m\rangle$ involved in this second-order transition. For an EQ transition the selection rules impose that $\Delta L = 0, \pm 2$ and that $\Delta M = 0, \pm 1, \pm 2$, by noting that the transition between two s states is forbidden [3]. Thus, the intermediate states leading to non-zero electric quadrupole transition moments are d states:

$$|m\rangle = |N_m; L_m = 2; M_m = 0, \pm 1, \pm 2\rangle \tag{III.4}$$

with $\{N_m, L_m, M_m\}$ their quantum numbers.

Given equation (III.2) the wavefunctions of these quantum states are written as

$$\begin{cases} \psi_e(\mathbf{r}) = R_{N_e,0}(r)\,Y_0^0 & \text{(III.5a)} \\ \psi_g(\mathbf{r}) = R_{N_g,0}(r)\,Y_0^0 & \text{(III.5b)} \\ \psi_m(\mathbf{r}) = R_{N_m,2}(r)\,Y_2^{M_m}(\theta,\varphi) \qquad \text{with } M_m = 0, \pm 1, \pm 2 & \text{(III.5c)} \end{cases}$$

where the excited and ground state wavefunctions have no angular dependencies, and thus are states with a spherical symmetry.

Now that all the wavefunctions of the involved states in this second-order transition are determined, we can calculate the electric quadrupole transition moment corresponding, first, to the transition between the excited and the intermediate states:

$$Q_{ij}^{em} = \langle e|Q_{ij}|m\rangle \tag{III.6a}$$
$$= -\frac{e}{2}\int_{\mathbb{R}^3} R_{N_e,0}^*(r)\left(Y_0^0\right)^*\left(x_i x_j - r^2\frac{\delta_{ij}}{3}\right) R_{N_m,2}(r)\,Y_2^{M_m}(\theta,\varphi)\,\mathrm{d}^3 r \tag{III.6b}$$
$$= -\frac{e}{2}\int_0^\infty r^4 R_{N_e,0}^*(r) R_{N_m,2}(r)\,\mathrm{d}r \int_{4\pi}\left(Y_0^0\right)^*\left(\frac{x_i x_j}{r^2} - \frac{\delta_{ij}}{3}\right) Y_2^{M_m}(\theta,\varphi)\,\mathrm{d}\Omega \tag{III.6c}$$

with $\mathrm{d}\Omega$ the element of solid angle and where the traceless form of the electric quadrupole moment operator $Q_{ij} = -\frac{e}{2}\left(x_i x_j - r^2\frac{\delta_{ij}}{3}\right)$ has been used [4]. Notice that the radial integral depends only on the principal quantum numbers, while the angular integrals depend solely on the magnetic quantum number of the intermediate states M_m.

Calculation of the angular integrals

Let us now calculate the angular integrals. To this end we use the complex conjugate and the orthonormality properties of the harmonic spherical functions [5]:

$$\left(Y_L^M(\theta,\varphi)\right)^* = (-1)^M Y_L^{-M}(\theta,\varphi), \tag{III.7a}$$

$$\int_{4\pi} \left(Y_L^M(\theta,\varphi)\right)^* Y_{L'}^{M'}(\theta,\varphi)\,\mathrm{d}\Omega = \delta_{LL'}\,\delta_{MM'}. \tag{III.7b}$$

By using the last property we notice directly that the term

$$\int_{4\pi} \left(Y_0^0\right)^* \frac{\delta_{ij}}{3} Y_2^{M_m}(\theta,\varphi)\,\mathrm{d}\Omega \tag{III.8}$$

vanishes. Thus, we still have to calculate the following integral for the five possible values of M_m:

$$\int_{4\pi} \left(Y_0^0\right)^* \frac{x_i x_j}{r^2} Y_2^{M_m}(\theta,\varphi)\,\mathrm{d}\Omega = (-1)^{M_m} \frac{1}{\sqrt{4\pi}} \int_{4\pi} \frac{x_i x_j}{r^2} \left(Y_2^{-M_m}(\theta,\varphi)\right)^* \mathrm{d}\Omega \tag{III.9}$$

where we used $Y_0^0 = \frac{1}{\sqrt{4\pi}}$ and the complex conjugate property.

To simplify the calculations the idea is to express the products $x_i x_j/r^2$ as a function of the spherical harmonics [5]:

$$\begin{cases} \dfrac{x^2}{r^2} = \dfrac{\sqrt{4\pi}}{3} Y_0^0 - \dfrac{1}{3}\sqrt{\dfrac{4\pi}{5}} Y_2^0 + \sqrt{\dfrac{2\pi}{15}} \left(Y_2^2 + Y_2^{-2}\right) & \text{(III.10a)} \\ \dfrac{y^2}{r^2} = \dfrac{\sqrt{4\pi}}{3} Y_0^0 - \dfrac{1}{3}\sqrt{\dfrac{4\pi}{5}} Y_2^0 - \sqrt{\dfrac{2\pi}{15}} \left(Y_2^2 + Y_2^{-2}\right) & \text{(III.10b)} \\ \dfrac{z^2}{r^2} = \dfrac{\sqrt{4\pi}}{3} Y_0^0 + \dfrac{2}{3}\sqrt{\dfrac{4\pi}{5}} Y_2^0 & \text{(III.10c)} \\ \dfrac{xy}{r^2} = i\sqrt{\dfrac{2\pi}{15}} \left(Y_2^{-2} - Y_2^2\right) & \text{(III.10d)} \\ \dfrac{yz}{r^2} = i\sqrt{\dfrac{2\pi}{15}} \left(Y_2^{-1} + Y_2^1\right) & \text{(III.10e)} \\ \dfrac{xz}{r^2} = \sqrt{\dfrac{2\pi}{15}} \left(Y_2^{-1} - Y_2^1\right). & \text{(III.10f)} \end{cases}$$

Thus, for each value of M_m and by using the orthonormality property, the non-zero integrals can be easily identified and calculated. By doing so one shows that

$$Q_{ij}^{em} = q^{em} S_{ij}^{M_m} \tag{III.11}$$

with

$$q^{em} := -\frac{e}{2\sqrt{30}} \int_0^\infty r^4 R_{N_e,0}^*(r) R_{N_m,2}(r)\,\mathrm{d}r \tag{III.12}$$

which depends only on the principal quantum numbers N_e and N_m, and with the second-rank tensors $\mathbf{S}^{M_m}$

$$\mathbf{S}^{-2} := \begin{pmatrix} 1 & -i & 0 \\ -i & -1 & 0 \\ 0 & 0 & 0 \end{pmatrix}, \quad \mathbf{S}^{-1} := \begin{pmatrix} 0 & 0 & 1 \\ 0 & 0 & -i \\ 1 & -i & 0 \end{pmatrix}, \quad \mathbf{S}^{0} := \sqrt{\frac{2}{3}} \begin{pmatrix} -1 & 0 & 0 \\ 0 & -1 & 0 \\ 0 & 0 & 2 \end{pmatrix}, \quad \mathbf{S}^{1} := \begin{pmatrix} 0 & 0 & -1 \\ 0 & 0 & -i \\ -1 & -i & 0 \end{pmatrix}, \quad \mathbf{S}^{2} := \begin{pmatrix} 1 & i & 0 \\ i & -1 & 0 \\ 0 & 0 & 0 \end{pmatrix} \tag{III.13}$$

which depend solely on the quantum number M_m.

Similar developments lead to

$$Q_{ij}^{mg} = q^{mg} \left(S_{ij}^{M_m}\right)^*. \tag{III.14}$$

Conclusion

We can now calculate the fourth-rank tensor $\boldsymbol{\mathcal{Q}}^{eg}(\omega_\alpha, \omega_{\alpha'})$, given in equation (III.1), where the summation runs over all possible intermediate states, defined here by the quantum numbers N_m et M_m (L_m is fixed to 2)[1]:

$$\boldsymbol{\mathcal{Q}}^{eg}(\omega_\alpha, \omega_{\alpha'}) = \sum_{N_m}\sum_{M_m}\left\{\frac{q^{em}\mathbf{S}^{M_m}q^{mg}\left(\mathbf{S}^{M_m}\right)^*}{\omega_{em}-\omega_\alpha} + \frac{q^{mg}\left(\mathbf{S}^{M_m}\right)^*q^{em}\mathbf{S}^{M_m}}{\omega_{em}-\omega_{\alpha'}}\right\} \tag{III.15a}$$

$$= \sum_{N_m} q^{em}q^{mg}\left\{\frac{\sum\limits_{M_m}\mathbf{S}^{M_m}\left(\mathbf{S}^{M_m}\right)^*}{\omega_{em}-\omega_\alpha} + \frac{\sum\limits_{M_m}\left(\mathbf{S}^{M_m}\right)^*\mathbf{S}^{M_m}}{\omega_{em}-\omega_{\alpha'}}\right\} \tag{III.15b}$$

We can show $\forall i,j,k,l = 1,2,3$ that

$$\sum_{M_m} S_{ij}^{M_m}\left(S_{kl}^{M_m}\right)^* = \sum_{M_m}\left(S_{ij}^{M_m}\right)^* S_{kl}^{M_m} = 2\left(\delta_{ik}\delta_{jl} + \delta_{il}\delta_{jk} - \frac{2}{3}\,\delta_{ij}\delta_{kl}\right). \tag{III.16}$$

Thus, the tensor can be rewritten as

$$\mathcal{Q}_{ijkl}^{eg}(\omega_\alpha, \omega_{\alpha'}) = 2\sum_{N_m} q^{em}q^{mg}\left(\frac{1}{\omega_{em}-\omega_\alpha} + \frac{1}{\omega_{em}-\omega_{\alpha'}}\right)\left(\delta_{ik}\delta_{jl} + \delta_{il}\delta_{jk} - \frac{2}{3}\,\delta_{ij}\delta_{kl}\right) \tag{III.17}$$

and its normalized version is given by

$$\hat{\mathcal{Q}}_{ijkl}^{eg}(\omega_\alpha, \omega_{\alpha'}) := \frac{\mathcal{Q}_{ijkl}^{eg}(\omega_\alpha, \omega_{\alpha'})}{\|\boldsymbol{\mathcal{Q}}^{eg}(\omega_\alpha, \omega_{\alpha'})\|} = \frac{1}{\sqrt{20}}\left(\delta_{ik}\delta_{jl} + \delta_{il}\delta_{jk} - \frac{2}{3}\,\delta_{ij}\delta_{kl}\right) \tag{III.18}$$

that is independent of the frequencies of the emitted quanta and where the norm of an n^{th} rank tensor $\mathbf{U}$ with $n \in \mathbb{N}_0$ has been defined as $\|\mathbf{U}\|^2 := \sum_{i_1,i_2,\ldots,i_n} |U_{i_1,i_2,\ldots,i_n}|^2$.

By using the modified Voigt notation introduced in the main text and in the previous section, the second-order electric quadrupole transition moment can be rewritten as a second-rank tensor in five dimensions:

$$\hat{\boldsymbol{\mathcal{Q}}}^{eg} := \frac{\boldsymbol{\mathcal{Q}}^{eg}}{\|\boldsymbol{\mathcal{Q}}^{eg}\|} = \frac{1}{\sqrt{20}}\begin{pmatrix} 4/3 & -2/3 & 0 & 0 & 0 \\ -2/3 & 4/3 & 0 & 0 & 0 \\ 0 & 0 & 1 & 0 & 0 \\ 0 & 0 & 0 & 1 & 0 \\ 0 & 0 & 0 & 0 & 1 \end{pmatrix} \tag{III.19}$$

[1] Y. Muniz, F. S. S. da Rosa, C. Farina, D. Szilard, and W. J. M. Kort-Kamp, Quantum two-photon emission in a photonic cavity, Physical Review A **100**, 023818 (2019).

[2] C. Cohen-Tannoudji, B. Diu, and F. Laloë, *Quantum mechanics. Volume 1: Basic concepts, tools, and applications*, second edition ed. (Wiley-VCH Verlag GmbH & Co. KGaA, Weinheim, 2020).

[3] R. D. Cowan, *The theory of atomic structure and spectra*, Los Alamos series in basic and applied sciences No. 3 (University of California Press, Berkeley, 1981).

[4] L. Novotny and B. Hecht, *Principles of Nano-Optics*, 2nd ed. (Cambridge University Press, Cambridge, 2012).

[5] G. B. Arfken, H.-J. Weber, and F. E. Harris, *Mathematical methods for physicists: a comprehensive guide*, 7th ed. (Elsevier, Amsterdam ; Boston, 2013).

[1] The energy of the intermediate states does not depend on M_m [2].